

รายการอ้างอิง

- [1] J. Ogrodzki. Circuit Simulation Methods and Algorithms. USA.: CRC Press, 1994.
- [2] K. David and C. Ward. Numerical Analysis: Mathematics of Scientific Computer. USA.: BROOKS/COLE, 2002.
- [3] G. L. Wilson and K. A. Schmidt. Transmission Line Models for Switching Studies: Design Criteria II. Selection of Section Length, Model Design and Tests. IEEE Transactions on Power Apparatus and Systems PAS-93,1 (1974): 389-395.
- [4] D. M. Triesenberg. An Efficient State Variable Transmission Line Model. IEEE Transactions on Power Apparatus and Systems PAS-98,2 (1979): 484-492.
- [5] F. H. Branin, Jr. Transient analysis of lossless transmission lines. Proceedings of the IEEE 55,11 (1967): 2012-2013.
- [6] W. S. Meyer and H. W. Dommel. Numerical Modelling of Frequency-Dependent Transmission-Line Parameters in an Electromagnetic Transients Program. IEEE Transactions on Power Apparatus and Systems PAS-93,5 (1974): 1401-1409.
- [7] J. R. Marti. Accurate Modelling of Frequency-Dependent Transmission Lines in Electromagnetic Transient Simulations. IEEE Transactions on Power Apparatus and Systems PAS-101,1 (1982): 147-157.
- [8] F. Y. Chang. The generalized method of characteristics for waveform relaxation analysis of lossy coupled transmission lines. Microwave Theory and Techniques, IEEE Transactions on 37,12 (1989): 2028-2038.
- [9] J. George A. Baker and P. Graves-Morris. Pade Approximants. USA.: Addison-Wesley Publishing, 1981.
- [10] J. S. Roychowdhury, A. R. Newton and D. O. Pederson. An impulse-response based linear time-complexity algorithm for lossy interconnect simulation. IEEE International Conference on Computer-Aided Design, ICCAD-91 1, (1991): 62-65.
- [11] S. Lin and E. S. Kuh. Transient simulation of lossy interconnects based on the recursive convolution formulation. Circuits and Systems I: Fundamental

- Theory and Applications, IEEE Transactions on [see also Circuits and Systems I: Regular Papers, IEEE Transactions on] 39,11 (1992): 879-892.
- [12] K. Gallivan, E. Grimme and P. V. Dooren. Asymptotic waveform evaluation via Lanczos methods. Appl. Math Letter 7, (1994): 75-80.
- [13] J. R. Griffith and M. S. Nakhla. Time-domain analysis of lossy coupled transmission lines. Microwave Theory and Techniques, IEEE Transactions on 38,10 (1990): 1480-1487.
- [14] S. L. Manney, M. S. Nakhla and Z. Qi-Jun. Analysis of nonuniform, frequency-dependent high-speed interconnects using numerical inversion of Laplace transform. Computer-Aided Design of Integrated Circuits and Systems, IEEE Transactions on 13,12 (1994): 1513-1525.
- [15] T. K. Tang and M. S. Nakhla. Analysis of high-speed VLSI interconnects using the asymptotic waveform evaluation technique. Computer-Aided Design of Integrated Circuits and Systems, IEEE Transactions on 11,3 (1992): 341-352.
- [16] S. K. Das and W. T. Smith. Application of asymptotic waveform evaluation for analysis of skin effect in lossy interconnects. Electromagnetic Compatibility, IEEE Transactions on 39,2 (1997): 138-146.
- [17] A. Odabasioglu, M. Celik and L. T. Pileggi. PRIMA: passive reduced-order interconnect macromodeling algorithm. Computer-Aided Design of Integrated Circuits and Systems, IEEE Transactions on 17,8 (1998): 645-654.
- [18] W. T. Beyene. Pole-clustering and rational-interpolation techniques for simplifying distributed systems. Circuits and Systems I: Fundamental Theory and Applications, IEEE Transactions on [see also Circuits and Systems I: Regular Papers, IEEE Transactions on] 46,12 (1999): 1468-1472.
- [19] K. Ogata. Modern Control Engineering. USA.: Prentice-Hall, 1998.
- [20] Avant Corporation. Star-Hspice Manual. CA: Avant Corporation, 1998.
- [21] D. B. Kuznetsov and J. E. Schutt-Aine. Optimal transient simulation of transmission lines. Circuits and Systems I: Fundamental Theory and Applications, IEEE Transactions on [see also Circuits and Systems I: Regular Papers, IEEE Transactions on] 43,2 (1996): 110-121.

ภาคผนวก

ภาคผนวก ก.**บทความทางวิชาการที่ได้รับการตีพิมพ์**

1. **บทความที่ได้รับการตีพิมพ์ในวารสารวิชาการในระดับนานาชาติ**

Panuwat Dan-klang and Ekachai Leelarasmee, "Simulation of Voltage and Current Distributions in Transmission Lines using State Variables and Exponential Approximation", ETRI Journal, Volume 31, Number 1, February 2009, pp 42-50

2. **บทความที่ได้รับการตอบรับตีพิมพ์ในวารสารวิชาการในระดับนานาชาติ**

Panuwat Dan-klang and Ekachai Leelarasmee, "Transient Simulation of Voltage and Current Distributions within Transmission Lines", IEICE TRANS. ELECTRON., VOL.E92-C, No.4, April 2009

3. **บทความที่ถูกรับเสนอในการประชุมวิชาการระดับนานาชาติ**

Panuwat Dan-klang and Ekachai Leelarasmee, "Transient Simulation of Coupled Transmission Lines based on Piecewise Exponential Approximation of Voltage and Current Distributions", Asia-Pacific Microwave Conference (APMC 2007), Bangkok Thailand , December 11 – 14, 2007, pp. 1051-1054

Simulation of Voltage and Current Distributions in Transmission Lines Using State Variables and Exponential Approximation

Panuwat Dan-Klang and Ekachai Leelarasme

A new method for simulating voltage and current distributions in transmission lines is described. It gives the time domain solution of the terminal voltage and current as well as their line distributions. This is achieved by treating voltage and current distributions as distributed state variables (DSVs) and turning the transmission line equation into an ordinary differential equation. Thus the transmission line is treated like other lumped dynamic components, such as capacitors. Using backward differentiation formulae for time discretization, the DSV transmission line component is converted to a simple time domain companion model, from which its local truncation error can be derived. As the voltage and current distributions get more complicated with time, a new piecewise exponential with controllable accuracy is invented. A segmentation algorithm is also devised so that the line is dynamically bisected to guarantee that the total piecewise exponential error is a small fraction of the local truncation error. Using this approach, the user can see the line voltage and current at any point and time freely without explicitly segmenting the line before starting the simulation.

Keywords: Exponential approximation, piecewise interpolation distributed state variable, transmission line.

Manuscript received Sept. 12, 2008; revised Dec. 17, 2008; accepted Dec. 24, 2008.
This work was supported by the Thailand Research Fund and Chulalongkorn University Ratchadapiseksompoj Fund, Thailand.
Panuwat Dan-Klang (phone: +662 218 6488, email: epanuwatd@gmail.com) and Ekachai Leelarasme (email: ekachai@chula.ac.th) are with the Electrical Engineering Department, Chulalongkorn University, Patumwan, Bangkok, Thailand.

I. Introduction

A transmission line, as shown in Fig. 1, is an important component found in both power and communication distribution networks. It also appears in electrical circuits in various forms such as microstrips, coaxial cables, and high-speed interconnects in integrated circuits. At low frequency, the line can be treated as being short circuited or replaced by lumped components. However, for high-frequency applications, such as high-voltage spike and high-speed communication, the line can have a significant effect on the dynamic of the circuit with which the line is connected. Hence, a transient simulation that treats a transmission line as a dynamic component must be developed. The dynamic equation is usually described by the telegraph equation [1], which consists of a set of linear partial differential equations comprising both temporal and spatial derivatives of line voltages and currents:

$$\begin{aligned}\frac{\partial v(x,t)}{\partial x} &= -L \frac{\partial i(x,t)}{\partial t} - Rv(x,t), \\ \frac{\partial i(x,t)}{\partial x} &= -C \frac{\partial v(x,t)}{\partial t} - Gi(x,t).\end{aligned}\quad (1)$$

Such a formulation significantly differs from lumped components, that is, capacitor and inductor, which are described only by differential equations, such as $i = C(dv/dt)$ or $v = L(di/dt)$. Hence, the telegraph equation does not fit with the equation formulation procedure of conventional circuit simulators, such as Hspice [2], EMTP [3], and MultiSim [4]. Moreover, its frequency domain terminal characteristic is an irrational function of the complex frequency s . Thus, the line

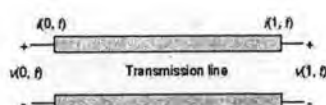
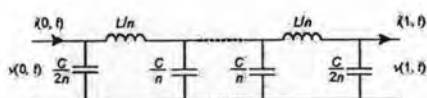


Fig. 1. Transmission line model.

Fig. 2. Transmission line modeled as n segments of lumped components.

terminals cannot be accurately modeled by a finite number of lumped components. An exact calculation of its transient response is impossible except for some special cases, such as $R=0$ and $G=0$ [1].

During the past three decades, various methods have been developed to approximate the dynamic of the distributed state line to allow the transient solution of the transmission line circuit to be numerically computable. The methods can be classified according to the selected domain of approximation, namely, frequency or spatial approximation.

The frequency approximation methods focus on approximating the terminal frequency responses of a transmission line with rational functions that has a finite number of poles. They are usually referred to as model order reduction (MOR) [5] methods. The simplest method of this class is the segmentation method, which replaces a transmission line with a large number (e.g. 100) of segments of lumped R , L , G , and C components as shown in Fig. 2. More efficient and accurate MOR methods have been proposed, such as PRIMA [6], [7] and DOMMEL [8], [9].

Frequency approximation methods have been shown to reduce the complexity of computing the time domain companion model of a transmission line. However, once the approximation is carried out, the original telegraph equation is no longer used in the transient analysis. That is, the reduced model is determined *a priori*. Hence, even if the time discretization, that is, the backward differentiation formula [10], is carried out using very small time steps, the transient solution of a transmission line circuit will converge only to that of the reduced frequency model, not the original one. Furthermore, there is no explicit formula for determining the time domain error or accuracy of the frequency methods. Therefore, time accuracy control is not possible. Another disadvantage of the frequency approximation method is that only the transient results at the terminal ends of the line are calculated. If the user

needs to find the transient at some internal points within the line, he/she has to divide the line at those points into several segments before starting the simulation.

The spatial approximation methods derive the time domain companion model directly from the telegraph equation. Two examples are the state-based [11] and the semi-discretization [12] methods. This companion model was shown to depend on the voltage and current distributions along the line at previous time points. Since the telegraph equation is used within the time iteration loop, the transient solution can converge to the exact solution as the time step is reduced. Unfortunately, the exact line voltage and current distributions cannot be analytically described; therefore, they must be approximated in the spatial domain by simple functions. Both the state-based and semi-discretization methods propose piecewise linear approximation. Moreover, they do not provide concrete details of the mechanism for controlling the accuracy of the piecewise linear approximation. Therefore, it is not clear whether its transient solution can be theoretically guaranteed to converge to the exact solution as the time step is reduced to increase transient accuracy.

This paper describes a variation of the distributed state variable (DSV) method for handling a transmission line in the time domain. The method was first introduced in [13]. It is a spatial approximation method, but it differs significantly from other previously mentioned methods in its derivation and implementation procedures. In the DSV method, line voltage and current distributions are treated as the state variables of the transmission line and are called DSVs. The telegraph equation can be transformed into a first-order state equation in terms of these DSVs. Thus, conventional backward differentiation techniques can be directly applied in the same way as other lumped dynamic components, such as capacitors and inductors. The method also gives the time domain companion model of a transmission line along with the formula to compute its local truncation error (LTE). This LTE is used to determine the appropriate time step. However, it will be shown that the DSVs become more complicated with time and more computationally expensive to track. To simplify these distributions, the piecewise exponential (PWE) function is proposed to be used where appropriate. However, the accuracy of this spatial approximation method is controlled by the computed LTE. The transient solution of the transmission line circuit can converge to the exact solution as the time step decreases because the LTE will also decrease. One advantage is that the line voltage and current distributions at all times are calculated and can be stored. Thus, users can view these distributions at any time or point without having to divide the line and restart the simulation.

This paper is organized as follows. The basic concept of the DSV method is given in section II. In section III, the PWE

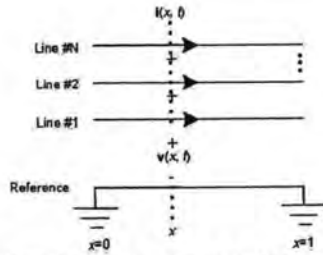


Fig. 3. $N+1$ coupled transmission line with the bottom line treated as a reference.

approximation is introduced to simplify these distributions at each time point and its error formula is derived. An algorithm which dynamically divides the transmission line into several segments is also described. A rigorous criterion for controlling the approximation errors that depend on the LTE is also suggested. Several examples are given in section IV to demonstrate how the method works.

II. Distributed State Variable

The type of transmission line considered in this paper is a set of $N+1$ coupled uniform transmission lines with the unit length as shown in Fig. 3.

Let the bottom line be treated as a reference line. The dynamic behavior of the other lines with respect to the reference line can be described by the telegraph equation as

$$\frac{\partial}{\partial x} \begin{bmatrix} \mathbf{v}(x,t) \\ \mathbf{i}(x,t) \end{bmatrix} = - \begin{bmatrix} 0 & \mathbf{L} \\ \mathbf{C} & 0 \end{bmatrix} \frac{\partial}{\partial t} \begin{bmatrix} \mathbf{v}(x,t) \\ \mathbf{i}(x,t) \end{bmatrix} - \begin{bmatrix} 0 & \mathbf{R} \\ \mathbf{G} & 0 \end{bmatrix} \begin{bmatrix} \mathbf{v}(x,t) \\ \mathbf{i}(x,t) \end{bmatrix}, \quad (2)$$

where $\mathbf{v}(x,t)$ and $\mathbf{i}(x,t)$ are vectors of N voltage and current distributions at distance x and time t with respect to the reference line, \mathbf{L} , \mathbf{C} , \mathbf{R} , and \mathbf{G} are $N \times N$ matrices of inductance, capacitance, resistance, and conductance measured as per unit distance and with respect to the reference line. To implement our analysis approach, the telegraph equation (2) can be formulated as

$$\frac{\partial}{\partial t} \begin{bmatrix} \mathbf{v}(x,t) \\ \mathbf{i}(x,t) \end{bmatrix} = -\mathbf{A}^{-1} \left(\mathbf{B} + \mathbf{I} \frac{\partial}{\partial x} \right) \begin{bmatrix} \mathbf{v}(x,t) \\ \mathbf{i}(x,t) \end{bmatrix}, \quad (3)$$

$$\text{where } \mathbf{A} = \begin{bmatrix} 0 & \mathbf{L} \\ \mathbf{C} & 0 \end{bmatrix} \text{ and } \mathbf{B} = \begin{bmatrix} 0 & \mathbf{R} \\ \mathbf{G} & 0 \end{bmatrix}.$$

If we simply treat $\partial/\partial x$ as an operator, then (3) can be viewed as an ordinary differential equation or state equation with $\begin{bmatrix} \mathbf{v}(x,t) \\ \mathbf{i}(x,t) \end{bmatrix}$ as its state. Therefore, we call $\begin{bmatrix} \mathbf{v}(x,t) \\ \mathbf{i}(x,t) \end{bmatrix}$ the

DSV of the transmission line, and we call (3) the DSV formulation of the telegraph equation. This formulation allows us to treat the whole set of coupled transmission lines as a single dynamic component in the same way as we treat a capacitor or an inductor because they are all described by state equations. Therefore, all numerical steps used to deal with capacitors and inductors in the transient simulation can be applied directly to the transmission line. That is, the time derivative of its state variable must first be discretized by the well known backward differentiation formula [11]. In this paper, we shall apply the backward Euler differentiation formula with time step $h_n = t_n - t_{n-1}$ to approximate the time derivative in (3) at time t_n as

$$\frac{1}{h_n} \begin{bmatrix} \mathbf{v}_n(x) \\ \mathbf{i}_n(x) \end{bmatrix} - \begin{bmatrix} \mathbf{v}_{n-1}(x) \\ \mathbf{i}_{n-1}(x) \end{bmatrix} = -\mathbf{A}^{-1} \left(\mathbf{B} + \mathbf{I} \frac{\partial}{\partial x} \right) \begin{bmatrix} \mathbf{v}_n(x) \\ \mathbf{i}_n(x) \end{bmatrix}, \quad (4)$$

where $\begin{bmatrix} \mathbf{v}_n(x) \\ \mathbf{i}_n(x) \end{bmatrix}$ is the approximated solution of $\begin{bmatrix} \mathbf{v}(x,t_n) \\ \mathbf{i}(x,t_n) \end{bmatrix}$,

and $\begin{bmatrix} \mathbf{v}(x,0) \\ \mathbf{i}(x,0) \end{bmatrix}$ is the vector of the initial line voltage and

current distributions. Without loss of generality, we assume that

$$\begin{bmatrix} \mathbf{v}(x,0) \\ \mathbf{i}(x,0) \end{bmatrix} = 0 \text{ for all } x \in [0,1]. \text{ Note that (4) is a recursive}$$

equation describing the distribution at t_n in terms of its previous value at t_{n-1} . After some algebraic manipulation, this equation can be rewritten as

$$\frac{d}{dx} \begin{bmatrix} \mathbf{v}_n(x) \\ \mathbf{i}_n(x) \end{bmatrix} = \mathbf{M}_n \begin{bmatrix} \mathbf{v}_n(x) \\ \mathbf{i}_n(x) \end{bmatrix} + \mathbf{D}_n \begin{bmatrix} \mathbf{v}_{n-1}(x) \\ \mathbf{i}_{n-1}(x) \end{bmatrix}, \quad (5)$$

where $\mathbf{M}_n = -\left[\frac{\mathbf{A}}{h_n} + \mathbf{B} \right]$ and $\mathbf{D}_n = \frac{\mathbf{A}}{h_n}$.

The recursive property of (5) can be combined from 0 to t_n in the following matrix form:

$$\frac{d\mathbf{y}(x)}{dx} = \mathbf{\Gamma} \mathbf{y}(x), \quad (6)$$

where

$$\mathbf{y}(x) = \begin{bmatrix} \mathbf{v}_1(x) \\ \mathbf{i}_1(x) \\ \mathbf{v}_2(x) \\ \mathbf{i}_2(x) \\ \vdots \\ \mathbf{v}_n(x) \\ \mathbf{i}_n(x) \end{bmatrix} \text{ and } \mathbf{\Gamma} = \begin{bmatrix} \mathbf{M}_1 & 0 & 0 & 0 \\ \mathbf{D}_2 & \mathbf{M}_2 & 0 & 0 \\ 0 & \ddots & \ddots & \vdots \\ 0 & 0 & \mathbf{D}_n & \mathbf{M}_n \end{bmatrix}. \quad (7)$$

From this, the solution of (6) can be solved to obtain

$$\begin{aligned} \begin{bmatrix} \mathbf{v}_n(x) \\ \mathbf{i}_n(x) \end{bmatrix} &= [0, \dots, \mathbf{I}] e^{Y_n x} \mathbf{y}(0) \\ &= [\psi_1(x), \dots, \psi_{n-1}(x), e^{M_n x}] \mathbf{y}(0). \end{aligned} \quad (8)$$

This equation can be rewritten as

$$\begin{bmatrix} \mathbf{v}_n(x) \\ \mathbf{i}_n(x) \end{bmatrix} = \exp(\mathbf{M}_n x) \begin{bmatrix} \mathbf{v}_n(0) \\ \mathbf{i}_n(0) \end{bmatrix} + \Psi_n(x), \quad x \in [0, 1], \quad (9)$$

where

$$\Psi_n(x) = \sum_{i=1}^{n-1} \psi_i(x) \begin{bmatrix} \mathbf{v}_i(0) \\ \mathbf{i}_i(0) \end{bmatrix}. \quad (10)$$

With $x = 1$, we obtain the following relationship between the line terminal voltages and currents:

$$\begin{bmatrix} \mathbf{v}_n(1) \\ \mathbf{i}_n(1) \end{bmatrix} = \exp(\mathbf{M}_n) \begin{bmatrix} \mathbf{v}_n(0) \\ \mathbf{i}_n(0) \end{bmatrix} + \Psi_n(1). \quad (11)$$

This equation describes the time domain companion model of the transmission line with respect to its terminals on both ends, where $\Psi_n(1)$ is a constant term whose calculating formula is described in the appendix. To comply with the nodal equation formulation, we perform some matrix operations and obtain the following input admittance matrix of the transmission line as well as its model given in Fig. 4:

$$\begin{bmatrix} \mathbf{i}_n(0) \\ \mathbf{i}_n(1) \end{bmatrix} = \mathbf{Z}_n^{-1} \begin{bmatrix} (\tanh(\Lambda_n))^{-1} - (\sinh(\Lambda_n))^{-1} \\ (\sinh(\Lambda_n))^{-1} - (\tanh(\Lambda_n))^{-1} \end{bmatrix} \begin{bmatrix} \mathbf{v}_n(0) \\ \mathbf{v}_n(1) \end{bmatrix} + \begin{bmatrix} \mathbf{J}_0 \\ \mathbf{J}_1 \end{bmatrix}, \quad (12)$$

where \mathbf{Z}_n and Λ_n are such that

$$\Lambda_n = \begin{bmatrix} \mathbf{I} & \mathbf{Z}_n \\ \mathbf{I} & -\mathbf{Z}_n \end{bmatrix}^{-1} \begin{bmatrix} -\Lambda_n & 0 \\ 0 & \Lambda_n \end{bmatrix} \begin{bmatrix} \mathbf{I} & \mathbf{Z}_n \\ \mathbf{I} & -\mathbf{Z}_n \end{bmatrix},$$

$$\begin{bmatrix} \mathbf{J}_0 \\ \mathbf{J}_1 \end{bmatrix} = \mathbf{Z}_n^{-1} (\exp(\Lambda_n) - \exp(-\Lambda_n))^{-1} \begin{bmatrix} \mathbf{I} & \mathbf{I} \\ \exp(\Lambda_n) & \exp(-\Lambda_n) \end{bmatrix} \Psi_n(1),$$

where $\mathbf{Y}_2 = \mathbf{Z}_n^{-1} \sinh^{-1}(\Lambda_n)$ and $\mathbf{Y}_1 = \mathbf{Y}_2 - \mathbf{Z}_n^{-1} \tanh^{-1}(\Lambda_n)$.

A standard circuit simulator can then use this companion model along with the companion models of other components, such as capacitors and inductors to set up the circuit matrix equation at time t_n . Once, the circuit equation is solved, $\mathbf{v}_n(0)$, $\mathbf{i}_n(0)$, $\mathbf{v}_n(1)$, and $\mathbf{i}_n(1)$ can be used to determine the distribution $\begin{bmatrix} \mathbf{v}_n(x) \\ \mathbf{i}_n(x) \end{bmatrix}$ according to the differential equation in (4). The DSV approach also allows the calculation of the LTE of the line as

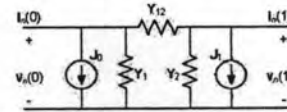


Fig. 4. Companion model of transmission line at both ends.

$$LTE_n = \left\| \begin{bmatrix} \mathbf{v}_n(x) \\ \mathbf{i}_n(x) \end{bmatrix} - \begin{bmatrix} \hat{\mathbf{v}}_n(x) \\ \hat{\mathbf{i}}_n(x) \end{bmatrix} \right\|, \quad (13)$$

where $\begin{bmatrix} \hat{\mathbf{v}}_n(x) \\ \hat{\mathbf{i}}_n(x) \end{bmatrix}$ is the predicted value of $\begin{bmatrix} \mathbf{v}_n(x) \\ \mathbf{i}_n(x) \end{bmatrix}$. Here, the norm is defined by

$$\|\mathbf{y}(\cdot)\|^2 \equiv \int_0^1 \mathbf{y}^T(x) \mathbf{T}^T \mathbf{T} \mathbf{y}(x) dx, \quad (14)$$

where \mathbf{T} is a $2N \times 2N$ non-singular matrix used to weigh the voltage and current distributions. Since the first-order backward differentiation formula is used in the time discretization, the predicted value should be the first-order forward differentiation formula [8], that is,

$$\begin{bmatrix} \hat{\mathbf{v}}_n(x) \\ \hat{\mathbf{i}}_n(x) \end{bmatrix} = \begin{bmatrix} \mathbf{v}_{n-1}(x) \\ \mathbf{i}_{n-1}(x) \end{bmatrix} + \frac{h_n}{h_{n-1}} \left\{ \begin{bmatrix} \mathbf{v}_{n-1}(x) \\ \mathbf{i}_{n-1}(x) \end{bmatrix} - \begin{bmatrix} \mathbf{v}_{n-2}(x) \\ \mathbf{i}_{n-2}(x) \end{bmatrix} \right\}. \quad (15)$$

The actual procedure for computing LTE_n is given in the appendix. The computed LTE of the line is then used to determine the next time step, $t_{n+1} = t_n + \Delta t_n$, along with the LTE of the other lumped dynamic components.

III. Piecewise Exponential Approximation

To study the computation complexity of the DSV method, we note that \mathbf{M}_n is a $2N \times 2N$ matrix. It follows that $\begin{bmatrix} \mathbf{v}_n(x) \\ \mathbf{i}_n(x) \end{bmatrix}$

has $2Nn$ exponential terms. Thus, the total computational complexity of the DSV at time t_n is of the order $\sum_{i=1}^n 2Ni = Nn(n+1)$. Moreover, the DSV method that we described in (8) must store all past values of voltage and current at $x=0$, that is, $\begin{bmatrix} \mathbf{v}_i(0) \\ \mathbf{i}_i(0) \end{bmatrix}; i = 1, \dots, N-1$ in order to obtain $\begin{bmatrix} \mathbf{v}_n(x) \\ \mathbf{i}_n(x) \end{bmatrix}$ according

to (9). This fast growing rate of computation and storage requirement is a serious drawback. To alleviate this problem at t_{n+1} , we propose to approximate $\begin{bmatrix} \mathbf{v}_n(x) \\ \mathbf{i}_n(x) \end{bmatrix}$ with a simplified

function $\begin{bmatrix} \hat{\mathbf{v}}_n(x) \\ \hat{\mathbf{i}}_n(x) \end{bmatrix}$ of the following form:

$$\begin{bmatrix} \hat{v}_s(x) \\ \hat{i}_s(x) \end{bmatrix} = \exp(\hat{M}x) \begin{bmatrix} v_s(x) \\ i_s(x) \end{bmatrix} \approx \begin{bmatrix} v_s(x) \\ i_s(x) \end{bmatrix}. \quad (16)$$

Once \hat{M} is obtained, the calculation of $w_{n+1}(x)$ becomes

$$\frac{d}{dx} \begin{bmatrix} \hat{v}_s(x) \\ \hat{i}_s(x) \\ v_{n+1}(x) \\ i_{n+1}(x) \end{bmatrix} = \begin{bmatrix} \hat{M} & 0 \\ D_{n+1} & M_{n+1} \end{bmatrix} \begin{bmatrix} \hat{v}_s(x) \\ \hat{i}_s(x) \\ v_{n+1}(x) \\ i_{n+1}(x) \end{bmatrix}, \quad (17)$$

which is much simpler than using (7) or (8).

A good strategy for finding \hat{M} would be to let $\begin{bmatrix} \hat{v}_s(x) \\ \hat{i}_s(x) \end{bmatrix}$ interpolate $\begin{bmatrix} v_s(x) \\ i_s(x) \end{bmatrix}$ as much as possible. Therefore, we choose $2N+1$ interpolating points evenly distributed within the segment, that is,

$$x_i = \frac{i}{2N}, \quad i = 0, 1, \dots, 2N.$$

Substituting x_i in (16), we have

$$\exp(\hat{M}i/2N) \begin{bmatrix} v_s(0) \\ i_s(0) \end{bmatrix} = \begin{bmatrix} v_s(\frac{i}{2N}) \\ i_s(\frac{i}{2N}) \end{bmatrix}, \quad i = 1, \dots, 2N. \quad (18)$$

Because it is an exponential function, it can be deduced that

$$\exp(\hat{M}i/2N) \begin{bmatrix} v_s(\frac{i-1}{2N}) \\ i_s(\frac{i-1}{2N}) \end{bmatrix} = \begin{bmatrix} v_s(\frac{i}{2N}) \\ i_s(\frac{i}{2N}) \end{bmatrix}, \quad i = 1, \dots, 2N. \quad (19)$$

In matrix form, this becomes

$$\exp(\hat{M}/2N) W_0 = W_1, \quad (20)$$

where

$$W_0 = \begin{bmatrix} v_s(0) & v_s(\frac{1}{2N}) & \dots & v_s(\frac{2N-1}{2N}) \\ i_s(0) & i_s(\frac{1}{2N}) & \dots & i_s(\frac{2N-1}{2N}) \end{bmatrix},$$

and

$$W_1 = \begin{bmatrix} v_s(\frac{1}{2N}) & v_s(\frac{2}{2N}) & \dots & v_s(\frac{2N}{2N}) \\ i_s(\frac{1}{2N}) & i_s(\frac{2}{2N}) & \dots & i_s(\frac{2N}{2N}) \end{bmatrix}.$$

Thus,

$$\hat{M} = 2N \ln(W_1 W_0^{-1}). \quad (21)$$

To maintain accuracy with respect to the transient simulation,

the approximating function is accepted only when $\begin{bmatrix} \hat{v}_s(x) \\ \hat{i}_s(x) \end{bmatrix}$ is close to $\begin{bmatrix} v_s(x) \\ i_s(x) \end{bmatrix}$ within a small percentage of its local truncation error. Therefore, the criteria for accepting the approximation is

$$ERR = \left\| \begin{bmatrix} \hat{v}_s(x) \\ \hat{i}_s(x) \end{bmatrix} - \begin{bmatrix} v_s(x) \\ i_s(x) \end{bmatrix} \right\| < \alpha LTE_s, \text{ where } \alpha \ll 1.$$

Otherwise, the approximation is not successful, and the segment is divided into two halves using a bisection algorithm, each of which is approximated by its own exponential function using the techniques described above. This time, the errors of the two segments are added before they are tested. If they still fail the test, only the segment that has the largest error will be divided. At the same time two adjacent segments may be combined if their error is acceptable. Hence, we are now ready to suggest the following segmentation algorithm.

Step 1. Set $K=1$ and $\alpha \ll 1$. That is, treat the whole line as one segment.

Step 2. Compute \hat{M}_i and ERR_i , $i = 1, \dots, K$.

Step 3. Calculate $ERR = \sqrt{\sum_{i=1}^K ERR_i^2}$.

Step 4. If $ERR \leq \alpha \cdot LTE_s$, exit.

Step 5. Determine \hat{i} such that

$$ERR_{\hat{i}} = \max(ERR_i, i = 1, \dots, K)$$

Step 6. Divide the \hat{i} -th segment into two at its middle point.

Step 7. Set $K=K+1$ and go to step 2.

IV. Numerical Examples

The DSV with the piecewise exponential approximation (PEA) methods has been tested with 5 transmission line circuits using MATLAB to verify the calculations. Where applicable, all results are compared with a standard circuit simulator, Hspice [2]. The first circuit, shown in Fig. 5, consists of 4 uncoupled lossy transmission lines. The parameters of each transmission line are $L=1$ mH/m, $C=1$ μ F/m, $G=0$ S/m, and $R=1$ Ω /m. Each line is one meter long and starts with zero voltage and current distributions. Its unit step input has a 0.1 ms rise time. This circuit is simulated using 0.5 mV local truncation error, and the approximation error factor is $\alpha=0.1$. The simulated waveform at the load-end of line 1 is shown in Fig. 6. It is indistinguishable from the results of Hspice [2]. Figure 7 shows how the lines are segmented dynamically, and the maximum number of segments is 15. However, this number gradually decreases to 1 segment when the line

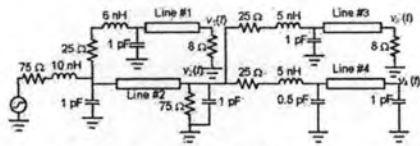


Fig. 5. Circuit diagram of 4 uncoupled lossy transmission lines (0.1 ms).

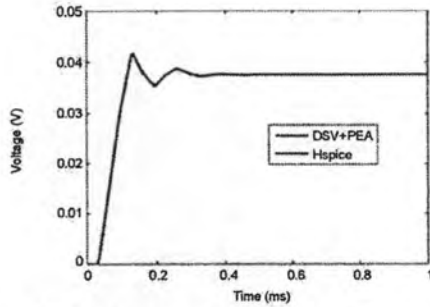


Fig. 6. Voltage waveform at the $v_1(t)$ of the circuit in Fig. 5. Allowable local truncation error is 0.5 mV, and approximation error factor α is 0.1.

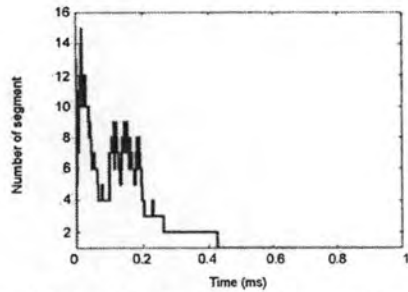


Fig. 7. Variation of number of exponential segments with time of line 1 of the circuit shown in Fig. 5 at various time points.

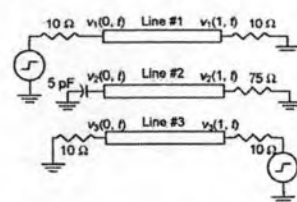


Fig. 8. Circuit comprising 3 lossy transmission lines.

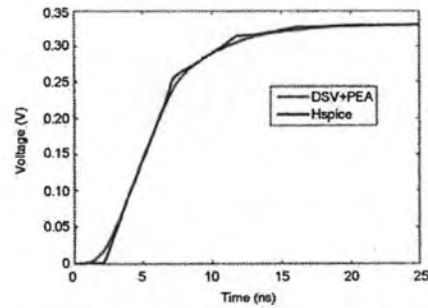


Fig. 9. Simulated waveform at the right end of the top line of the circuit in Fig. 8. Allowable local truncation error is 0.5 mV, and approximation error α is 0.1.

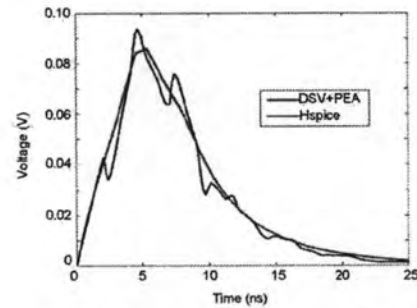


Fig. 10. Voltage waveform at $v_2(1, t)$ of the circuit shown in Fig. 8.

activities reach the DC steady state; therefore, the execution time can be fast.

The circuit in the second example, shown in Fig. 8, consists of three joined transmission lines ($N=3$). The lines are 1 meter long with the following parameters:

$$R = \begin{bmatrix} 10 & 0 & 0 \\ 0 & 10 & 0 \\ 0 & 0 & 10 \end{bmatrix} \Omega/m, \quad G = \begin{bmatrix} 1 & 0 & 0 \\ 0 & 1 & 0 \\ 0 & 0 & 1 \end{bmatrix} \text{mS/m},$$

$$L = \begin{bmatrix} 100 & 25 & 2.5 \\ 25 & 100 & 25 \\ 2.5 & 25 & 100 \end{bmatrix} \text{nH/m}, \quad C = \begin{bmatrix} 50 & -10 & -1 \\ -10 & 60 & -10 \\ -1 & -10 & 50 \end{bmatrix} \text{pF/m}.$$

The circuit has two unit step inputs, one at the top line and the other at the bottom line. The rise time of each unit step input is 5 ns. The circuit is simulated using 0.5 mV maximum local truncation error, and the approximation error factor is $\alpha=0.1$.

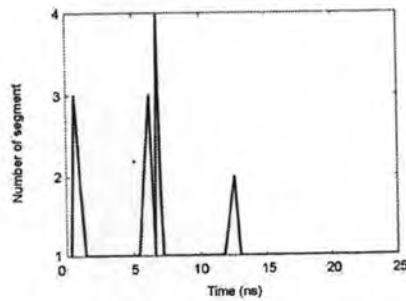


Fig. 11. Variation of number of exponential segments with time of the circuit in Fig. 8.

The simulated waveforms at $v_1(1, t)$ and $v_2(1, t)$ are shown in Figs. 9 and 10 and agree very well with those of Hspice. Figure 11 shows only the number of segments used by our method, indicating fast computation.

In the last example, we demonstrate the advantage of the DSV method that voltage and current distribution can be obtained simultaneously. This event cannot be obtained in a standard circuit simulation such as Hspice without segmenting the line before starting the simulation. This last example circuit, shown in Fig. 12, comprises three transmission lines with a fault within line 1. The line is 1 meter long and has the following distributed parameters:

$$L = \begin{bmatrix} 100 & 25 & 2.5 \\ 25 & 100 & 25 \\ 2.5 & 25 & 100 \end{bmatrix} \text{ nH/m}, \quad G = \begin{bmatrix} 1 & 0 & 0 \\ 0 & 1 & 0 \\ 0 & 0 & 1 \end{bmatrix} \text{ mS/m},$$

$$C = \begin{bmatrix} 50 & -10 & -1 \\ -10 & 60 & -10 \\ -1 & -10 & 50 \end{bmatrix} \text{ pF/m}, \quad R = \begin{bmatrix} 1 & 0 & 0 \\ 0 & 1 & 0 \\ 0 & 0 & 1 \end{bmatrix} \text{ } \Omega/\text{m}.$$

A fault occurs at $x=0.7$ m and at 0.4 ps in the form of a 0.4 A current pulse with a 0.2 ps pulse-width, which is about 10% of the transmission time delay. The distribution voltage across line 2 is shown in Fig. 13.

V. Conclusion

The DSV for time domain simulation of circuit transmission lines has been presented. It transforms the telegraph equation into a state equation that allows the use of conventional techniques to obtain its transient response as well as local truncation error. The PEA method was also introduced to reduce the computational complexity of the DSV method. An algorithm based on a bisection scheme was introduced to segment the line

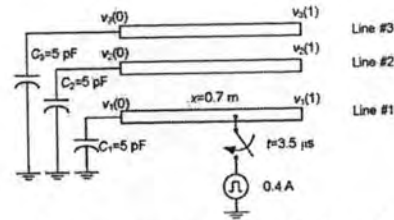


Fig. 12. Circuit comprising 3 lossy transmission lines with fault occurring on one line.

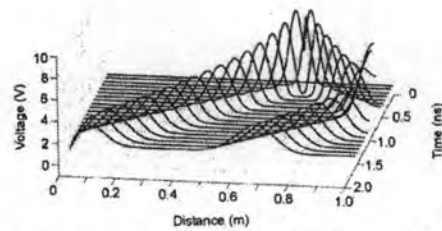


Fig. 13. Line 2 voltage distribution of circuit shown in Fig. 12.

dynamically so that the approximation error is small compared to the local truncation error. Numerical examples showed that this combined DSV-PEA method works very well and requires a small number of segments; therefore, this method can be computationally efficient. However, the calculations of the local truncation error as well as the approximating functions and error require complex matrix calculations such as those shown in the appendix. No CPU time comparison with existing circuit simulations was carried out, and we do not expect our method to execute faster. The key advantages of this method are that its accuracy can be automatically adjusted based on the user specified value of the local truncation error and that the voltage and current distribution can also be obtained without extra calculation or explicit segmentation of a line.

Finally, we give here a short remark about how forward and reflect waves can be computed as by-products of the simulation output.

Forward wave: $V^+(s) = \frac{1}{2}[V_1(s) + Z_c(s)I_1(s)]$ (22)

Reflected wave: $V^-(s) = \frac{1}{2}[V_2(s) + Z_c(s)I_2(s)]$ (23)

Here, $Z_c(s) = \sqrt{(Ls + R)(Cs + G)^{-1}}$.

By performing the inverse Laplace transform, these two equations become

$$v^+(t) = \frac{1}{2} [v_1(t) + z_c(t) * i_1(t)], \tag{24}$$

$$v^-(t) = \frac{1}{2} [v_2(t) + z_c(t) * i_2(t)], \tag{25}$$

where $z_c(t) * i_1(t)$ and $z_c(t) * i_2(t)$ are the convolution integrals, which can be time consuming. However, since $Z_c(s)$ is known, it is possible to invert $Z_c(s)$ by using Padé approximation [14] which accurately approximates $Z_c(s)$ with a rational function. Partial fraction expansion can be applied to this rational function which can then be inverted. Then, the convolution term can be carried out recursively [15], yielding the required forward and reflected waves at any time point. Note that the time step for recursive convolution can be the same as that used by the DSV method. In that case, the two processes can be carried out in parallel.

Appendix 1.

Lemma 1. This lemma will be needed in A2 and A3.

Let T and M be matrices of appropriate dimensions. Then,

$$\int_0^1 e^{Mx} T^T T e^{Mx} dx = e^{-M} \begin{bmatrix} 0 & I \\ I^T & M^T \end{bmatrix} \begin{bmatrix} I \\ 0 \end{bmatrix},$$

where I is an identity matrix of the same dimension as M .

Proof: Let $F(x) = e^{\begin{bmatrix} -M & 0 \\ T^T T & M \end{bmatrix} x} = \begin{bmatrix} e^{-Mx} & 0 \\ Q(x) & e^{Mx} \end{bmatrix}$.

Then, $\frac{d}{dx} F(x) = \begin{bmatrix} -M & 0 \\ T^T T & M \end{bmatrix} \begin{bmatrix} e^{-Mx} & 0 \\ Q(x) & e^{Mx} \end{bmatrix}$

$$= \begin{bmatrix} -M e^{-Mx} & 0 \\ \frac{d}{dx} Q(x) & M e^{Mx} \end{bmatrix},$$

from which we have

$$\frac{d}{dx} Q(x) = T^T T e^{-Mx} + M Q(x) \text{ with } Q(0) = 0.$$

The solution of this differential equation at $x = 1$ is

$$Q(1) = e^M \int_0^1 e^{-Mx} T^T T e^{Mx} dx.$$

Hence, $\int_0^1 e^{-Mx} T^T T e^{Mx} dx = e^{-M} Q(1)$.

Substitute $Q(1)$ from the definition of $F(x)$ to end the proof. \square

Appendix 2. Numerical Formula for Computing LTE_n in (13)

From (13) and (15), we have

$$LTE_n = \left\| \mathbf{w}_n(\cdot) - \left(1 + \frac{h_n}{h_{n-1}}\right) \mathbf{w}_{n-1}(\cdot) + \frac{h_n}{h_{n-1}} \mathbf{w}_{n-2}(\cdot) \right\|.$$

Using the definition in A1, we can rewrite LTE_n as

$$LTE_n = \left\| \mathbf{L} \mathbf{y}(\cdot) \right\| = \left\| \mathbf{L} e^{\Gamma x} \mathbf{y}(0) \right\|,$$

where $\mathbf{L} = \begin{bmatrix} 0 & \dots & 0 & \left(\frac{h_n}{h_{n-1}} - \mathbf{I}\right) & \left(-\mathbf{I} - \frac{h_n}{h_{n-1}} \mathbf{I}\right) & \mathbf{I} \end{bmatrix}$

Applying the definition of the norm in (12), we obtain

$$LTE_n^2 = \mathbf{y}(0)^T \int_0^1 e^{\Gamma x} \mathbf{L}^T \mathbf{T}^T \mathbf{T} \mathbf{L} e^{\Gamma x} dx \mathbf{y}(0).$$

Apply the result of lemma 1, and we have

$$LTE_n^2 = \mathbf{y}(0)^T \mathbf{Q} \mathbf{y}(0),$$

where $\mathbf{Q} = e^{-\Gamma} \begin{bmatrix} 0 & \mathbf{I} \\ \mathbf{I}^T \mathbf{T}^T \mathbf{T} \mathbf{L} & \mathbf{I}^T \end{bmatrix} \begin{bmatrix} \mathbf{I} \\ 0 \end{bmatrix}$, and \mathbf{I} is an identity matrix with the same dimension as Γ .

Appendix 3. Numerical Formula for Computing ERR_n

Based on the definitions in (7), let

$$\hat{\mathbf{y}}_n(x) = \begin{bmatrix} \mathbf{y}_n(x) \\ \hat{\mathbf{w}}_n(x) \end{bmatrix}, \hat{\Gamma} = \begin{bmatrix} \Gamma & 0 \\ 0 & \hat{M} \end{bmatrix}, \text{ and } \mathbf{L} = \begin{bmatrix} \mathbf{E}_n & -\mathbf{I} \end{bmatrix}.$$

Then, (7) and (14) can be combined to give

$$\hat{\mathbf{y}}_n(x) = e^{\hat{\Gamma}(x-x_{i-1})} \hat{\mathbf{y}}_n(x_{i-1}) \text{ for } x_{i-1} \leq x \leq x_i.$$

Also, ERR_n can be formulated as

$$ERR_n^2 = \int_{x_{i-1}}^{x_i} \left[\mathbf{L} \hat{\mathbf{y}}_n(x) \right]^T \mathbf{T}^T \mathbf{T} \left[\mathbf{L} \hat{\mathbf{y}}_n(x) \right] dx$$

$$= \hat{\mathbf{y}}_n(x_{i-1})^T \int_{x_{i-1}}^{x_i} e^{\hat{\Gamma}(x-x_{i-1})} \mathbf{L}^T \mathbf{T}^T \mathbf{T} \mathbf{L} e^{\hat{\Gamma}(x-x_{i-1})} dx \hat{\mathbf{y}}_n(x_{i-1})$$

$$= (x_i - x_{i-1}) \hat{\mathbf{y}}_n(x_{i-1})^T \int_0^1 e^{\hat{\Gamma} \tau} \mathbf{L}^T \mathbf{T}^T \mathbf{T} \mathbf{L} e^{\hat{\Gamma} \tau} d\tau \hat{\mathbf{y}}_n(x_{i-1})$$

$$= (x_i - x_{i-1}) \hat{\mathbf{y}}_n(x_{i-1})^T \mathbf{Q} \hat{\mathbf{y}}_n(x_{i-1}),$$

where $\mathbf{Q} = e^{-\hat{\Gamma}} \begin{bmatrix} 0 & \mathbf{I} \\ \mathbf{I}^T \mathbf{T}^T \mathbf{T} \mathbf{L} & \mathbf{I}^T \end{bmatrix} \begin{bmatrix} \mathbf{I} \\ 0 \end{bmatrix}$ and \mathbf{I} is an identity matrix with the same dimension as $\hat{\Gamma}$.

References

- [1] G. Miano and A. Maffucci, *Transmission Lines and Lumped Circuits*, Academic Press, 2001.
- [2] Avant Corporation, *Star-Hspice Manual*, Avant Corporation, CA, 1998.
- [3] M. Kizilcay, "Alternative Transients Program Features," 2008 [cited; Available from: <http://www.emtp.org/>].
- [4] National Instruments Corporation, NI Multisim, 2008 [cited July 10, 2008]; Available from: <http://www.ni.com/multisim/>.
- [5] A.C. Antoulas, *Approximation of Large-Scale Dynamical Systems*, SIAM Advances in Design and Control, 2005.
- [6] A. Odabasioglu, M. Celik, and L.T. Pileggi, "Prima: Passive Reduced-Order Interconnect Macromodeling Algorithm," *IEEE Trans. Computer-Aided Design of Integrated Circuits and Systems*, vol. 17, no. 8, 1998, pp. 645-654.
- [7] D. Saraswat, R. Achar, and M.S. Nakhla, "Passive Reduction Algorithm for RLC Interconnected Circuits with Embedded State-Space Systems (Press)," *IEEE Trans. Microwave Theory and Techniques*, vol. 52, no. 9, 2004, pp. 2215-2226.
- [8] H.W. Dommel, "Digital Computer Solution of Electromagnetic Transients in Single- and Multiphase Networks," *IEEE Trans. Power Apparatus and Systems*, vol. PAS-88, no. 4, 1969, pp. 388-399.
- [9] A. Ibrahim et al., "Transmission Line Model for Large Step Size Transient Simulations," *Proc. of the 1999 IEEE Canadian Conf. on Electrical and Computer Engineering*, vol. 2, 1999, pp. 1191-1194.
- [10] J. Ogrodzki, *Circuit Simulation Methods and Algorithms*, CRC Press, Inc., 1994.
- [11] Z. Tingdong, S.L. Dvorak, and J.L. Prince, "Lossy Transmission Line Simulation Based on Closed-Form Triangle Impulse Responses," *IEEE Trans. Computer-Aided Design of Integrated Circuits and Systems*, vol. 22, no. 6, 2003, pp. 748-755.
- [12] J.S. Roychowdhury, A.R. Newton, and D.O. Pederson, "Algorithms for the Transient Simulation of Lossy Interconnect," *IEEE Trans. Computer-Aided Design of Integrated Circuits and Systems*, vol. 13, no. 1, 1994, pp. 96-104.
- [13] E. Leelarasmee and P. Naenna, "A Distributed State Variables Approach to the Transmission Lines Transient Simulation," *Proc. the 2004 IEEE Asia-Pacific Conference on Circuits and Systems*, 2004, pp. 73-76.
- [14] G.A. Baker and P. G. Morris, *Pade' Approximant Part II: Extensions and Applications*, Addison-Wesley, 1981.
- [15] S. Lin and E.S. Kuh, "Transient Simulation of Lossy Interconnects Based on the Recursive Convolution Formulation," *IEEE Trans. Circuit and Systems*, vol. 39, no. 11, 1992, pp. 879-891.



Panuwat Dan-Klang received the BEng degree from Prince of Songkla University, Thailand, in 1998, and the MEng degree from Kasetsart University in 2005. Currently, he is a PhD student at Chulalongkorn University. His research interests include circuit simulation, digital IC design, and wireless sensor networks.



Ekachai Leelarasmee received his BEng degree in EE from Chulalongkorn University, Thailand, in 1974, and his PhD in EE from University of California, Berkeley, USA, in 1982, under the sponsorship of the Anandamahidol Foundation. For his PhD dissertation, in which waveform relaxation was first proposed and applied for time domain analysis of large scale MOS integrated circuits, he received three prestigious awards: the 1983 IEEE Guellemmin-Cauer Award, the 1982 IEEE/ACM Design Automation Conference Best Paper Award, and the 1981 U.C. Berkeley D.J. Sakrison Memorial Prize. He is now an associate professor with the Department of Electrical Engineering of Chulalongkorn University. He was the pioneering developer of Thailand's first circuit simulation program LEK, which won two invention awards from the National Research Council of Thailand in 1985 and 1988. His current research interests are circuit simulation programs, closed-caption TV systems, and VLSI designs.

PAPER

Transient Simulation of Voltage and Current Distributions within Transmission Lines

Panuwat DAN-KLANG^{1,a)} and Ekachai LEELARASMEE¹, Members

SUMMARY The problem of analyzing transient in transmission line circuits is studied with emphasis on obtaining the transient voltage and current distributions. A new method for solving Telegrapher equation that characterizes the uniform transmission lines is presented. It not only gives the time domain solution of the line terminal voltage and current, but also their distributions within the lines. The method achieves its goal by treating the voltage and current distributions as distributed state variables and transforms the Telegrapher equation into an ordinary differential equation. This allows the coupled transmission lines to be treated as a single component that behaves like other lumped dynamic components, such as capacitors and inductors. Using Backward Differentiation Formulae for time discretization, the transmission line component is converted to its time domain companion model, from which its local truncation error for time step control can be derived. As the shapes of the voltage and current distributions get more complicated with time, they can be approximated by piecewise exponential functions with controllable accuracy. A segmentation algorithm is thus devised so that the line is dynamically bisected to guarantee that the total piecewise exponential approximation error is only a small fraction of the local truncation error. Using this approach, the user can see the line voltage and current at any point and time freely without explicitly segment the line before starting the simulation.

Key words: exponential approximation, piecewise interpolation, distributed state variable, transmission line

1. Introduction

Transmission line, as shown in Fig. 1, is an important component for power distribution networks. It also appears in electrical circuits in various forms such as micro-strips, coaxial cables and high speed interconnects in integrated circuits. At low frequency, e.g. power line frequency, the line can be treated as being short circuited or replaced by lumped components. However, during transient such as high voltage spike or line fault, the line can have a significant effect on the dynamic of the circuit with which the line is connected. Hence, a transient algorithm that treats a transmission line as a dynamic component must be invented. For a uniform transmission line, the dynamic equation is usually described by the Telegrapher equation [1], which consists of a set of linear partial differential equations comprising both temporal and spatial derivatives of line voltages and currents. Such a formulation differs from lumped components, i.e. capacitor and inductor, which are only differential equations. Hence the Telegrapher Equation does not fit with the equation formulation procedure of conventional circuit

Manuscript received August 20, 2008.

Manuscript revised November 20, 2008.

¹The authors are with Electrical Engineering Department, Chulalongkorn University, Bangkok, 10330, Thailand.

a) E-mail: panuwat@digital.ce.eng.chula.ac.th

DOI: 10.1587/transle.E92.C.522

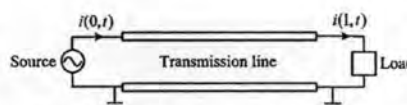


Fig. 1 Transmission line is used to link source and load to form a circuit.

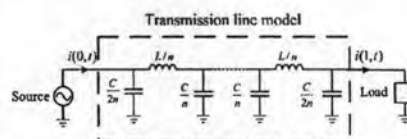


Fig. 2 Frequency approximation of a transmission line with lumped components.

simulators such as Hspice [2], EMTP [3] and MultiSim [4]. Moreover, its frequency domain terminal characteristic is an irrational function of the complex frequency s . Thus the line terminals cannot be accurately modelled by finite number of lumped components. An exact calculation of its transient response is impossible except for some special cases such as $R=0$ and $G=0$ [1]. During the past three decades, various methods were developed to approximate the dynamic of the transmission line in order to allow the transient solution of transmission line circuit numerically computable. They can be classified according to the selected domain of approximation, i.e. frequency and spatial approximation.

The frequency approximation methods focus on approximating the terminal frequency responses of a transmission line with rational functions that has finite number of poles. They are usually referred to as model order reduction or MOR [5] methods. The simplest method of this class is the segmentation method which replaces a transmission line with a large number (e.g. 100) of segments of lumped R,L,G,C components as shown in Fig. 2. A more efficient and accurate MOR method is presented by many researchers such as PRIMA [6] and DOMMEL [7].

The frequency approximation methods have been shown to reduce the complexity in computing the time domain companion model of a transmission line. However, once the approximation is carried out, the original Telegrapher Equation or measured data is no longer used in the transient analysis, i.e. the reduced model is determined a-priori. Hence, even if the time discretization, i.e. Backward Differ-

entiation Formula [8], is carried out using very small time steps, the transient solution of a transmission line circuit will converge only to that of the reduced frequency model, not the original one. Furthermore, there is no explicit formula for determining the time domain error or accuracy of the frequency methods. Therefore, accuracy control is not possible. Another disadvantage is that only the transient result at the terminal ends of the line are calculated. If the user needs to find the transient at some internal points within the line, he/she has to divide the line at those points into several sub lines before starting the simulation.

The spatial approximation methods derive the time domain companion model directly from the Telegrapher Equation. Two examples are the State-Based [9] and the Semi-Discretization [10] methods. This companion model was shown to depend on the voltage and current distributions along the line at previous but finite number of time points. Since the Telegrapher Equation is used within the time iteration loop, the transient solution can converge to the exact solution as the time step is reduced. Unfortunately, the exact line voltage and current distributions cannot be analytically described. Hence they must be approximated in the spatial domain by simple functions. Both the State-Based and Semi-Discretization methods proposed piecewise linear approximation. However, they did not provide a concrete detail about the mechanism for controlling the accuracy of the piecewise linear approximation. Therefore, it is not clear whether its transient solution can be guaranteed to converge to the exact solution as the time step is reduced for increasing transient accuracy.

This paper describes the Distributed State Variable (DSV) method for handling the transmission line in the time domain. The method is first introduced in [11]. It belongs to the spatial approximation method but significantly differs from other previously mentioned methods in its derivation and implementing procedures. In this method, line voltage and current distributions are treated as the state variables of the transmission line and called distributed state variables (DSV). Then the Telegrapher Equation can be transformed into a first order state equation in terms of these DSVs. Thus conventional Backward Differentiation techniques can be directly applied in the same way like other lumped dynamic components such as capacitors and inductors. It also gives the time domain companion model of a transmission line along with the formula for computing its local truncation error (LTE). This LTE is used to determine the appropriate time step. However, it will be shown that the DSVs get more complicated with time and become computationally expensive to keep track. To simplify these distributions, the piecewise exponential (PWE) function is used where appropriate. However, the accuracy of this spatial approximation is controlled by the computed LTE. Therefore, the transient solution of the transmission line circuit can converge to the exact solution as the time step is reduced since the LTE will also reduce. One advantage is that the line voltage and current distributions at all time points are calculated and can be stored. Thus user can view these distributions at any time or

point without having to divide the line and restart the simulation.

This paper is organized as follows. The basic concept of the DSV method is given in Sect. 2. In Sect. 3, the Piecewise Exponential (PWE) approximation is introduced to simplify these distributions at each time point and its error formula is derived. An algorithm that dynamically divides the transmission line into several segments is also described. A rigorous criterion for controlling the approximation errors that depends on the LTE is also suggested. Several examples are illustrated in Sect. 4 to show how the method works.

2. Distributed State Variable

Consider a set of $N + 1$ coupled uniform transmission lines with unit length as shown in Fig. 3.

Let the bottom line is treated as a reference line. Then the dynamic behavior of the other lines with respect to the reference line can be described by Telegrapher Equation as in (1).

$$\frac{\partial}{\partial x} \begin{bmatrix} v(x, t) \\ i(x, t) \end{bmatrix} = - \begin{bmatrix} 0 & \mathbf{L} \\ \mathbf{C} & 0 \end{bmatrix} \frac{\partial}{\partial t} \begin{bmatrix} v(x, t) \\ i(x, t) \end{bmatrix} - \begin{bmatrix} 0 & \mathbf{R} \\ \mathbf{G} & 0 \end{bmatrix} \begin{bmatrix} v(x, t) \\ i(x, t) \end{bmatrix} \quad (1)$$

where $v(x, t)$ and $i(x, t)$ are vectors of N voltage and current distributions at distance x and time t with respect to the reference line, \mathbf{L} , \mathbf{C} , \mathbf{R} and \mathbf{G} are $N \times N$ matrices of inductance, capacitance, resistance and conductance measured as per unit distance and with respect to the reference line. Our analysis approach defines $w(\bullet, t)$ such that

$$w(x, t) = \begin{bmatrix} v(x, t) \\ i(x, t) \end{bmatrix} \text{ for } x \in (0, 1) \text{ and } t \geq 0 \quad (2)$$

Then the Telegrapher Eq. (1) can be formulated in the following form

$$\frac{\partial}{\partial t} w(\bullet, t) = F(w(\bullet, t)) \quad (3)$$

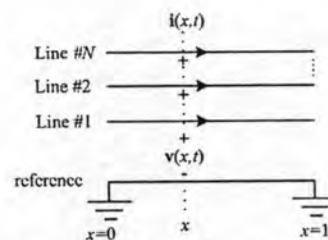


Fig. 3 Frequency approximation of a transmission line with lumped components.

524

where

$$F = -A^{-1} \left(B + I \frac{\partial}{\partial x} \right);$$

$$A = \begin{bmatrix} 0 & L \\ C & 0 \end{bmatrix} \text{ and } B = \begin{bmatrix} 0 & R \\ G & 0 \end{bmatrix} \quad (4)$$

This equation can be viewed as an ordinary differential equation or state equation with $w(\bullet, t)$ as its state. Therefore, we will call $w(\bullet, t)$ as the distributed state variable (DSV) of the transmission line and Eq. (3) as the DSV formulation of the Telegrapher Equation. This formulation allows us to treat the whole set of coupled transmission lines as a single dynamic component in the same way as we treat a capacitor or an inductor since they are all described by state equations. Hence all numerical steps used to deal with capacitors and inductors in the transient simulation can be applied directly to the transmission line. That is the time derivative of its state variable must first be discretized by the well known Backward Differentiation Formula (BDF) [8]. For ease of understanding in this paper, we shall apply the Backward Euler (BE) differentiation formula with time-step $h_n = t_n - t_{n-1}$ to approximate the time derivative in Eq. (3) at time t_n as follows

$$\frac{1}{h_n} [w_n(\bullet) - w_{n-1}(\bullet)] = F(w_n(\bullet)); \quad n = 1, 2, \dots \quad (5)$$

where $w_n(\bullet)$ is the approximated solution of $w(\bullet, t_n)$ with $w_0(\bullet) = w(\bullet, 0)$ which consists of the initial line voltage and current distributions. Without loss of generality, we assume that $w(x, 0) = 0$ for all $x \in (0, 1)$. Note that (5) is a recursive equation describing the distribution at t_n in terms of its previous value at t_{n-1} . Substituting from (4) into (5) we have

$$\frac{1}{h_n} [w_n(\bullet) - w_{n-1}(\bullet)] = -A^{-1} \left(B + I \frac{\partial}{\partial x} \right) w_n(\bullet)$$

After some algebraic manipulation, this equation can be rewritten as

$$\frac{d}{dx} w_n(x) = M_n w_n(x) + D_n w_{n-1}(x) \quad (6)$$

where $M_n = -\left[\frac{A}{h_n} + B \right]$ and $D_n = \frac{A}{h_n}$. Solving (6), that we explain in the appendix Appendix A, we obtain

$$w_n(x) = e^{M_n x} w_n(0) + \Psi_n(x); \quad x \in (0, 1) \quad (7)$$

where

$$\Psi_n(x) = \int_0^x e^{M_n(x-\tau)} D_n w_{n-1}(\tau) d\tau \quad (8)$$

With $x = 1$, we obtain the following relationship between the line terminal voltages and currents

$$w_n(1) = e^{M_n} w_n(0) + \Psi_n(1) \quad (9)$$

This equation describes the time domain companion

IEICE TRANS. ELECTRON., VOL.E92-C, NO.4 APRIL 2009

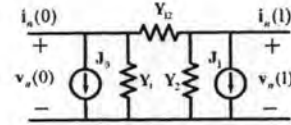


Fig. 4 A companion model of transmission line at both ends.

model of the transmission line with respect to its terminals on both ends. Where $\Psi_n(1)$ is a constant term whose calculating formula is described in the Appendix A. To comply with the nodal equation formulation which is described in the Appendix B, we perform some matrix operations and obtain the following input admittance matrix of the transmission line as well as its model in Fig. 4.

$$\begin{bmatrix} i_n(0) \\ i_n(1) \end{bmatrix} = Z_n^{-1} \begin{bmatrix} (\tanh(\Lambda_n))^{-1} & -(\sinh(\Lambda_n))^{-1} \\ (\sinh(\Lambda_n))^{-1} & -(\tanh(\Lambda_n))^{-1} \end{bmatrix} \times \begin{bmatrix} v_n(0) \\ v_n(1) \end{bmatrix} + \begin{bmatrix} J_0 \\ J_1 \end{bmatrix} \quad (10)$$

A standard circuit simulator can then use this companion model along with the companion models of other components such as capacitors and inductors to set up the circuit matrix equation at time t_n . Once, the circuit equation is solved, $v_n(0)$, $i_n(0)$, $v_n(1)$ and $i_n(1)$ can be used to determine the distribution $w_n(\bullet)$ according to (5). The DSV approach also allows the calculation of the local truncation error (LTE) of the line as follows.

$$LTE_n = \|w_n(\bullet) - \tilde{w}_n(\bullet)\| \quad (11)$$

where $\tilde{w}_n(\bullet)$ is the predicted value of $w_n(\bullet)$. The norm is defined by

$$\|y(\bullet)\|^2 \equiv \int_0^1 y^T(x) T^T T y(x) dx \quad (12)$$

where T is a $2N \times 2N$ non-singular matrix used to weigh the voltage and current distributions. Since the first order Backward Differentiation formula is used in the time discretization, the predicted value should be the first order Forward Differentiation formula [8], i.e.

$$\tilde{w}_n(\bullet) = w_{n-1}(\bullet) + \frac{h_n}{h_{n-1}} [w_{n-1}(\bullet) - w_{n-2}(\bullet)] \quad (13)$$

Actual procedure for computing LTE_n is shown in the appendix. The computed LTE of the line is then used to determine the next time step $h_{n+1} = t_{n+1} - t_n$ along with the LTE of the other lumped dynamic component.

3. Piecewise Exponential Approximation

To study the computation complexity of the DSV method, we let

$$y(x) = \begin{bmatrix} w_1(x) \\ w_2(x) \\ \vdots \\ w_n(x) \end{bmatrix} \text{ and } \Gamma = \begin{bmatrix} M_1 & 0 & 0 & 0 \\ D_2 & M_2 & 0 & 0 \\ 0 & \ddots & \ddots & \vdots \\ 0 & 0 & D_n & M_n \end{bmatrix} \quad (14)$$

Then Eq. (6) can be rewritten as $\frac{dy(x)}{dx} = \Gamma y(x)$. Thus we can write the solution in following form

$$w_n(x) = [0, \dots, I] e^{I x} y(0) \quad (15)$$

Since M_n is a $2N \times 2N$ matrix when N is number of transmission line except the reference line, it follows that $w_n(\bullet)$ has $2Nn$ exponential terms. Thus the total computational complexity of the DSV at time t_n is of the order $\sum_{i=1}^n 2Ni = Nn(n+1)$. Moreover, the DSV method must store all past values of voltage and current at $x = 0$, i.e. $w_i(0); i = 1, \dots, N-1$ in order to obtain $w_n(x)$ as shown in (15). This fast growing rate of computation and storage requirement is a serious drawback. To alleviate this problem at t_{n+1} , we approximate $w_n(x)$ with a simplified function $\hat{w}_n(x)$ of sufficient accuracy. One common approximation method is the piecewise linear interpolation. However, we feel that a piecewise linear function is not suitable because the line distributions, as given by (15), are always exponential functions. So, we propose to approximate the line distribution by a piecewise exponential function that has a smaller number of exponential terms than the original one. Hence, the $w_n(x)$ is approximated with $\hat{w}_n(x)$ by following form

$$\hat{w}_n(x) = e^{\hat{M}_n x} w_n(0) \approx w_n(x) \quad (16)$$

Once \hat{M} is obtained, the calculation of $w_{n+1}(x)$ becomes

$$\frac{d}{dx} \begin{bmatrix} \hat{w}_n(x) \\ w_{n+1}(x) \end{bmatrix} = \begin{bmatrix} \hat{M} & 0 \\ D_{n+1} & M_{n+1} \end{bmatrix} \begin{bmatrix} \hat{w}_n(0) \\ w_{n+1}(0) \end{bmatrix} \quad (17)$$

which is much simpler than using (15). A good strategy in finding \hat{M} would be to let $\hat{w}_n(x)$ interpolate $w_n(x)$ as much as possible. So, we choose $2N+1$ interpolating points evenly distributed within the segment, i.e.

$$x_i = \frac{i}{2N}; i = 0, 1, \dots, 2N$$

Hence

$$e^{\hat{M}_n i/2N} w_n(0) = w_n\left(\frac{i}{2N}\right); i = 1, \dots, 2N \quad (18)$$

By virtue of being exponential function, it can be deduced that

$$e^{\hat{M}_n i/2N} w_n\left(\frac{i-1}{2N}\right) = w_n\left(\frac{i}{2N}\right); i = 1, \dots, 2N \quad (19)$$

In matrix form, this becomes

$$e^{\hat{M}_n/2N} W_0 = W_1 \quad (20)$$

where

$$W_0 = \left[w_n(0), w_n\left(\frac{1}{2N}\right), \dots, w_n\left(\frac{2N-1}{2N}\right) \right]$$

and

$$W_1 = \left[w_n\left(\frac{1}{2N}\right), w_n\left(\frac{2}{2N}\right), \dots, w_n\left(\frac{2N}{2N}\right) \right]$$

Thus

$$\hat{M} = 2N \ln(W_1 W_0^{-1}) \quad (21)$$

To maintain accuracy with respect to the transient simulation, the approximating function will be accepted when the approximation function $\hat{w}(x)$ is close to the simulation result function $w_n(x)$ within a small percentage of its local truncation error, i.e. passing the following test

$$ERR = \|\hat{w}(\bullet) - w_n(\bullet)\| < \alpha LTE_n \text{ where } \alpha \ll 1 \quad (22)$$

Otherwise, the approximation is not successful and the segment must be divided into two halves, each of which is approximated by its own exponential function using the techniques described above. This time the errors of the two segments are added before being tested. If it still fails the test, only the segment that has the largest error will be divided. At the same time two adjacent segments may be combined if their error is acceptable. Hence we are now ready to suggest a segmentation algorithm as follows

- Step 1: Set $K = 1$ and $\alpha \ll 1$, i.e. treat the whole line as one segment.
- Step 2: Compute \hat{M}_i and $ERR_i; i = 1, \dots, K$.
- Step 3: Calculate $ERR = \sqrt{\sum_{i=1}^K ERR_i^2}$.
- Step 4: If $ERR \leq \alpha \cdot LTE_n$ then exit.
- Step 5: Determine \hat{i} such that $ERR_{\hat{i}} = \max(ERR_i; i = 1, \dots, K)$.
- Step 6: Divide the \hat{i} th segment into two at its middle point.
- Step 7: Set $K = K + 1$ and go to Step 2.

4. Numerical Examples

DSV with PEA methods has been tested with 5 transmission line circuits using MATLAB to perform the calculations. Unfortunately, it is impossible to make actual measurement for examples 3–5 as no such equipment exists. For the first two examples Hspice [2] is used as a reference solution. This is because Hspice uses difference approximation method for each transmission line problem to obtain optimal transient simulation algorithm [12]. Therefore its transient results are believed as a reference by many papers in this area. The first circuit, shown in Fig. 5, is a single transmission line with the following distributed parameters $L = 1 \text{ mH/m}$, $C = 10 \mu\text{F/m}$, $G = 0.02 \text{ S/m}$ and $R = 1 \Omega/\text{m}$. The line is 1 meter long and starts with zero voltage and current distributions. The applied input is a step voltage whose rise time is 0.1 msec and a time delay of 0.1 msec is expected

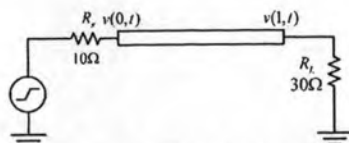


Fig. 5 A single transmission line circuit with unit step input having 0.1 msec rise time. The line delay time is around 0.1 msec.

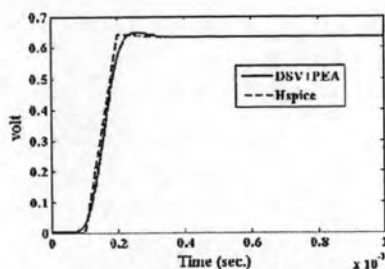


Fig. 6 The voltage waveform at the load-end of the circuit in Fig. 5. The allowable local truncation error is 0.5 mV and the approximation error factor α is 0.1.

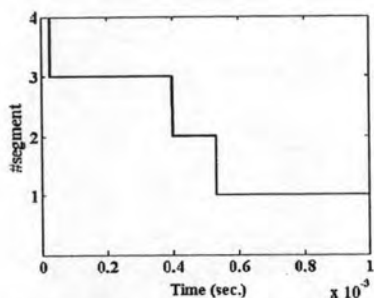


Fig. 7 Variation of #exponential segments used to simulate the circuit in Fig. 5 at different timepoints.

at the other end. The maximum local truncation error of 0.5 mV is allowed to control the time step which is adjusted dynamically from 0.2 μ sec to 0.4 μ sec. The piecewise exponential approximation error factor α is 0.1. The simulated voltage waveform at the load-end ($x = 1$) is shown as a solid line in Fig. 6. This waveform matches very well with the voltage waveform obtained from a well known commercial program Hspice [2], shown as a dotted line in the same figure. The well known smoothing effect of the Backward Euler formula is apparent from the graph. Figure 7 shows the number of exponential pieces required to approximate the distributions at various time points. We can see that our

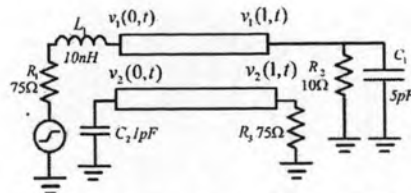


Fig. 8 A circuit to demonstrate the coupling effect of transmission lines. The unit step input has a 5 nsec rise time.

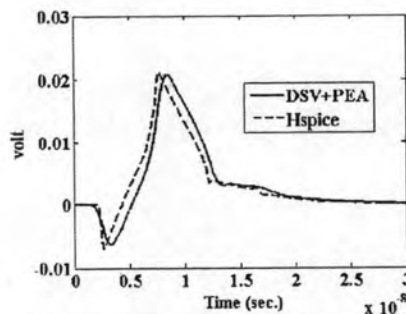


Fig. 9 The coupled waveform at the load-end of the bottom line of the circuit in Fig. 8.

method automatically and dynamically divides the line into a large number of segments while the unit step input wave travels in the line and gradually reduces the number of segments to 1 after the step input has reached the load and the whole line becomes fully charged.

The circuit in the second example, shown in Fig. 8, consists of two coupled transmission lines ($N = 2$). The lines are 1 meter long with the following parameters

$$\mathbf{R} = \begin{bmatrix} 10 & 0 \\ 0 & 10 \end{bmatrix} \Omega/\text{m} \quad \mathbf{G} = \begin{bmatrix} 1 & 0 \\ 0 & 1 \end{bmatrix} \text{mS}/\text{m}$$

$$\mathbf{L} = \begin{bmatrix} 100 & 25 \\ 25 & 100 \end{bmatrix} \text{nH}/\text{m} \quad \mathbf{C} = \begin{bmatrix} 50 & -10 \\ -10 & 60 \end{bmatrix} \text{pF}/\text{m}$$

The rise time of unit step input is 5 nsec. It is simulated using 0.5 mV maximum local truncation error and the approximation error factor is $\alpha = 0.1$. The simulated waveform at the load-end of the top line is almost indistinguishable from that obtained from Hspice. Figure 9 shows the simulated voltage waveform that is coupled from the top to bottom line at the load-end. The waveform also agrees quite well with Hspice. Figure 10 indicates that the maximum number of exponential segments used is only 7 which occurs only a few times while 2 or 3 segments are used most of the time.

The third circuit example, shown in Fig. 11, is a sin-

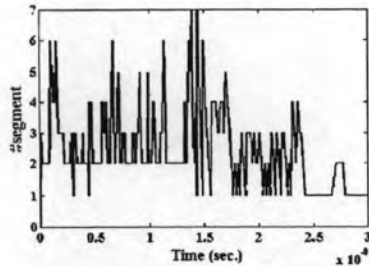


Fig. 10 Variation of exponential segments used to simulate the circuit of Fig. 8.

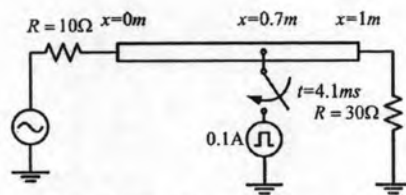


Fig. 11 A test circuit of insert current pulse at $x = 0.7$ m.

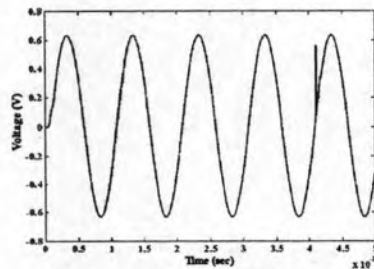


Fig. 12 The voltage waveform at $x = 0.7$ of circuit in Fig. 11.

gle transmission line with a fault occurred within the line. The line is 1 meter long and has the following distributed parameters $L = 1$ mH/m, $C = 10$ μ F/m, $G = 0.02$ S/m and $R = 1$ Ω /m. It is fed with sinusoidal voltage source with 1 Volt peak 1 kHz. A fault occurs at $x = 0.7$ m and at 4.1 msec in the form of 0.1 A current pulse with 5 μ sec pulse width as shown in Fig. 12. The voltage distribution during 4 msec to 4.17 msec is showed in Fig. 13 which shows the fault waveform split into two pulses that travel in the opposite direction. The maximum number of segment is 29 and occurs at the time of fault. Before and after this, the number of segments is 5 on average.

The fourth example is also a single line with fault that

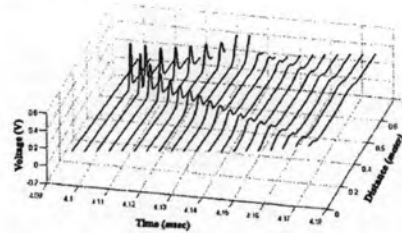


Fig. 13 A voltage distribution in the transmission line of circuit of Fig. 11 from 4 msec to 4.17 msec.

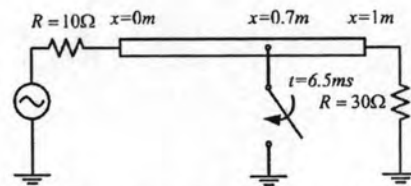


Fig. 14 A test circuit of ground fault occur at $x = 0.7$ m.

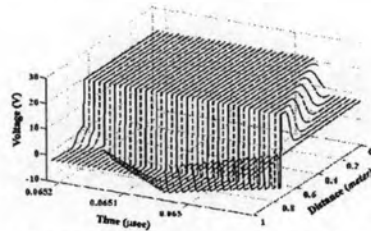


Fig. 15 The current distribution between 6.5 μ sec to 6.52 μ sec.

occurs as a line-to-ground short circuit in Fig. 14. The transmission line is fed with sinusoidal voltage source with 220 Volt peak 50 Hz. There is a ground fault at $x = 0.7$ m and $t = 6.5$ msec. The current distribution between 6.5 msec to 6.52 msec is shown in Fig. 15, and the variation of current at $x = 1$ is shown in Fig. 16.

The last circuit under test is shown in Fig. 17. It consists of three coupled transmission lines ($N = 3$). The lines are 1 meter long with the following parameters

$$L = \begin{bmatrix} 100 & 25 & 2.5 \\ 25 & 100 & 25 \\ 2.5 & 25 & 100 \end{bmatrix} \text{ nH/m}$$

$$C = \begin{bmatrix} 50 & -10 & -1 \\ -10 & 60 & -10 \\ -1 & -10 & 50 \end{bmatrix} \text{ pF/m}$$

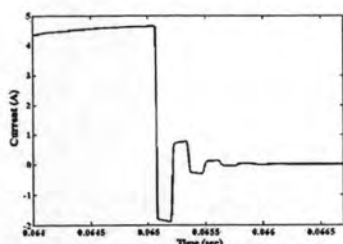


Fig. 16 Variation of current with time at $x = 1$ m of circuit in Fig. 15.

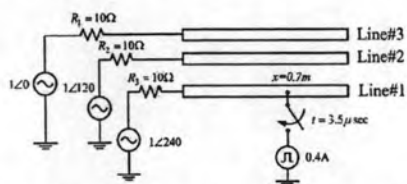


Fig. 17 A 3 phase lossy transmission lines with fault occurring on one line.

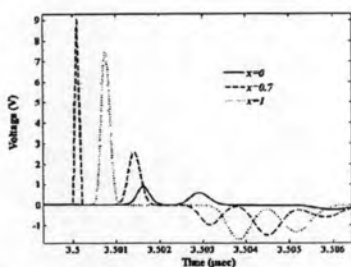


Fig. 18 The voltages at each distance point of Line#1 of circuit in Fig. 17

$$G = \begin{bmatrix} 1 & 0 & 0 \\ 0 & 1 & 0 \\ 0 & 0 & 1 \end{bmatrix} \text{ mS/m} \quad R = \begin{bmatrix} 1 & 0 & 0 \\ 0 & 1 & 0 \\ 0 & 0 & 1 \end{bmatrix} \Omega/\text{m}$$

The transmission lines are fed with 3 phase sinusoidal voltage source with 1 Volt peak 1 MHz. A fault occurs at $x = 0.7$ m and at $3.5 \mu\text{sec}$ in the form of 0.4 A current pulse with 20 psec pulse width. The voltages of Line#1 at three difference point, that are $x = 0$, $x = 0.7$ and $x = 1$, are shown in Fig. 18 and the coupled voltages from Line#1 to Line#2 are shown in Fig. 19. We show traveling waveform voltage between $3.5 \mu\text{sec}$ to $3.504 \mu\text{sec}$ of the Line#1 in Fig. 20 and the Line#2 in Fig. 21.

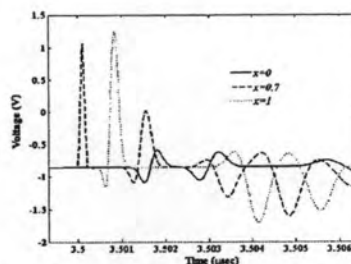


Fig. 19 The voltages at each distance point of Line#2 that coupling form Line#1.

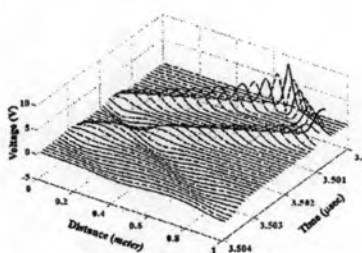


Fig. 20 A Line#1 voltage distribution between $3.5 \mu\text{sec}$ to $3.504 \mu\text{sec}$ of circuit of Fig. 17.

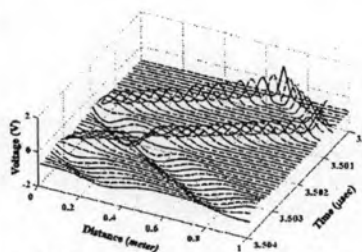


Fig. 21 A Line#2 voltage distribution between $3.5 \mu\text{sec}$ to $3.504 \mu\text{sec}$ of circuit of Fig. 17.

5. Conclusion

By treating the distributions of voltage and current as distributed state variables (DSV), a transmission line becomes an ordinary dynamic component. All numerical methods commonly used with a lumped dynamic component such as capacitor and inductor can also be applied to a transmission line, leading to its simple companion model as well as a formula for computing its local truncation error (LTE). How-

ever, its model evaluation requires accumulative knowledge of past distributions which must be approximated to reduce its computational complexity. The piecewise exponential approximation (PEA) is introduced for this purpose in which the distributions are approximated with functions having fewer exponential terms together with a formula for calculating its error. An algorithm based on a bisection scheme is introduced to segment the line dynamically in such a way that the approximation error is small compared to the local truncation error. Numerical examples have shown that this combined DSV-PEA method works very well and requires a small number of segments. Hence this method can be computationally efficient. However, the calculations of the local truncation error, the approximating functions and error require complex matrix calculations as shown in the appendix. The CPU time comparison with existing circuit simulations has not been carried out and we do not expect our method to execute faster. The key advantage of this method lies in the fact that its accuracy can be automatically adjusted based on the user specified value of the local truncation error and that the voltage and current distribution can also be obtained without extra calculation or explicitly segment the line. Whereas, the DVS is base on time discretized, this technique use small times step automatically for maintain accuracy in high frequencies circuit simulation. However, this effect is corresponding with the passive components thus this technique is still practical to use in high frequencies circuit simulation.

Acknowledgments

This work is supported by grants from Thailand Research Fund and Chulalongkorn University Ratchadapiseksompoj Fund.

References

- [1] G. Miano and A. Maffucci, *Transmission lines and Lumped Circuits*, Academic Press, 2001.
- [2] Avant Corporation, *Star-Inspector Manual*, Avant Corporation, CA, 1998.
- [3] <http://www.cmp.org/>
- [4] <http://www.ni.com/multisim/>
- [5] A.C. Antoulas, *Approximation of Large-Scale Dynamical Systems*, SIAM Advances in Design and Control, 2005.
- [6] A. Odubusioğlu, M. Celik, and L.T. Pileggi, "PRIMA: Passive reduced-order interconnect macromodeling algorithm," *IEEE Trans. Comput.-Aided Des. Integr. Circuits Syst.*, vol.17, no.8, pp.645-654, 1998.
- [7] H.W. Dommel, "Digital computer solution of electromagnetic transients in single-and multiphase network," *IEEE Trans. Power Appur. Syst.*, vol.PAS-88, no.4, pp.388-399, 1969.
- [8] J. Ogrodzki, *Circuit Simulation Methods and Algorithms*, CRC Press, 1994.
- [9] Z. Tingdong, S.L. Dvorak, and J.L. Prince, "Lossy transmission line simulation based on closed-form triangle impulse responses," *IEEE Trans. Comput.-Aided Des. Integr. Circuits Syst.*, vol.22, no.6, pp.748-755, 2003.
- [10] J.S. Roychowdhury, A.R. Newton, and D.O. Pederson, "Algorithms for the transient simulation of lossy interconnect," *IEEE Trans. Comput.-Aided Des. Integr. Circuits Syst.*, vol.13, no.1, pp.96-104, 1994.
- [11] E. Lechrasmecc and P. Nacma, "A distributed state variables approach to the transmission lines transient simulation," 2004 IEEE Asia-Pacific Conference on Circuits and Systems, vol.1, pp.73-76, 2004.
- [12] D.B. Kuznetsov and J.E. Schutt-Aid, "Optimal transient simulation of transmission lines," *IEEE Trans. Circuits Syst. I. Fundam. Theory Appl.*, vol.43, no.2, pp.110-121, 1996.

Appendix A: Numerical Formula for Computing in (7)

Define $y(x) \in \mathbb{R}^{2Nn}$, $\Gamma \in \mathbb{R}^{2Nm \times 2Nn}$, $I \in \mathbb{R}^{2Nn \times 2Nn}$ and $E_d \in \mathbb{R}^{2Nn \times 2Nn}$ such that

$$y(x) = \begin{bmatrix} w_1(x) \\ w_2(x) \\ \vdots \\ w_n(x) \end{bmatrix}, \Gamma = \begin{bmatrix} M_1 & 0 & 0 & 0 \\ D_2 & M_2 & 0 & 0 \\ 0 & \ddots & \ddots & \vdots \\ 0 & 0 & D_n & M_n \end{bmatrix}$$

I is an identity matrix and $E_d y(x) = w_f(x)$. Then we can rewrite (6) as $\frac{d}{dx} y(x) = \Gamma y(x)$. This gives

$$y(x) = e^{\Gamma x} y(0) \quad (\text{A-1})$$

Hence

$$\begin{aligned} w_n(x) &= E_n e^{\Gamma x} y(0) = E_n e^{\Gamma x} \sum_{i=1}^n E_i^T w_i(0) \\ &= e^{M_n x} w_n(0) + \Psi_n(x) \end{aligned} \quad (\text{A-2})$$

where

$$\Psi_n(x) = E_n e^{\Gamma x} \sum_{i=1}^{n-1} E_i^T w_i(0) \quad (\text{A-3})$$

$$= \begin{bmatrix} 0 & 0 & \cdots & 0 & I \end{bmatrix} e^{\Gamma x} \begin{bmatrix} w_1(0) \\ w_2(0) \\ \vdots \\ 0 \end{bmatrix} \quad (\text{A-4})$$

$$\text{Hence } \Psi_n(1) = \begin{bmatrix} 0 & 0 & \cdots & 0 & I \end{bmatrix} e^{\Gamma} \begin{bmatrix} w_1(0) \\ w_2(0) \\ \vdots \\ 0 \end{bmatrix}$$

Appendix B: Derivation of Transmission Line Companion Model in Nodal Form

In Sect. 2, we have

$$w_n(1) = e^{M_n} w_n(0) + \Psi_n(1)$$

$$\text{where } w_n(1) = \begin{bmatrix} v(1, t_n) \\ i(1, t_n) \end{bmatrix} \text{ and } w_n(0) = \begin{bmatrix} v(0, t_n) \\ i(0, t_n) \end{bmatrix}$$

The equation of transmission line companion model in nodal form can be written as

$$\begin{bmatrix} i_n(0) \\ i_n(1) \end{bmatrix} = Z_n^{-1} \begin{bmatrix} (\tanh(\Lambda_n))^{-1} & -(\sinh(\Lambda_n))^{-1} \\ (\sinh(\Lambda_n))^{-1} & -(\tanh(\Lambda_n))^{-1} \end{bmatrix}$$

$$\times \begin{bmatrix} \mathbf{v}_n(0) \\ \mathbf{v}_n(1) \end{bmatrix} + \begin{bmatrix} \mathbf{J}_0 \\ \mathbf{J}_1 \end{bmatrix} \quad (\text{A.5})$$

where \mathbf{Z}_n and Λ_n are such that

$$\mathbf{M}_n = \begin{bmatrix} \mathbf{I} & \mathbf{Z}_n \\ \mathbf{I} & -\mathbf{Z}_n \end{bmatrix}^{-1} \begin{bmatrix} -\Lambda_n & \mathbf{0} \\ \mathbf{0} & \Lambda_n \end{bmatrix} \begin{bmatrix} \mathbf{I} & \mathbf{Z}_n \\ \mathbf{I} & -\mathbf{Z}_n \end{bmatrix}$$

$$\text{and } \begin{bmatrix} \mathbf{J}_0 \\ \mathbf{J}_1 \end{bmatrix} = \mathbf{Z}_n^{-1} (e^{\Lambda_n} - e^{-\Lambda_n})^{-1} \begin{bmatrix} \mathbf{I} & \mathbf{I} \\ e^{\Lambda_n} & e^{-\Lambda_n} \end{bmatrix} \Psi_n(1)$$

This leads to the equivalent time domain companion model as shown in Fig. 4

$$\text{where } \mathbf{Y}_{12} = \mathbf{Z}_n^{-1} \sinh^{-1}(\Lambda_n)$$

$$\text{and } \mathbf{Y}_1 = \mathbf{Y}_2 = \mathbf{Z}_n^{-1} \tanh^{-1}(\Lambda_n) - \mathbf{Y}_{12}$$

Appendix C: Lemma 1: This Lemma Will Be Needed in Appendix D and Appendix E

Let \mathbf{T} and \mathbf{M} be matrices of appropriate dimensions. Then

$$\int_0^1 e^{\mathbf{M}^T x} \mathbf{T}^T \mathbf{T} e^{\mathbf{M}x} dx$$

$$= e^{-\mathbf{M}} \begin{bmatrix} \mathbf{0} & \mathbf{I} \end{bmatrix} e^{\begin{bmatrix} -\mathbf{M} & \mathbf{0} \\ \mathbf{T}^T \mathbf{T} & \mathbf{M} \end{bmatrix} x} \begin{bmatrix} \mathbf{I} \\ \mathbf{0} \end{bmatrix}$$

where \mathbf{I} is an identity matrix of the same dimension as \mathbf{M} .

Proof: Let $\mathbf{F}(x) = e^{\begin{bmatrix} -\mathbf{M} & \mathbf{0} \\ \mathbf{T}^T \mathbf{T} & \mathbf{M} \end{bmatrix} x} = \begin{bmatrix} e^{-\mathbf{M}x} & \mathbf{0} \\ \mathbf{Q}(x) & e^{\mathbf{M}x} \end{bmatrix}$

Then

$$\frac{d}{dx} \mathbf{F}(x) = \begin{bmatrix} -\mathbf{M} & \mathbf{0} \\ \mathbf{T}^T \mathbf{T} & \mathbf{M} \end{bmatrix} \begin{bmatrix} e^{-\mathbf{M}x} & \mathbf{0} \\ \mathbf{Q}(x) & e^{\mathbf{M}x} \end{bmatrix}$$

$$= \begin{bmatrix} -\mathbf{M}e^{-\mathbf{M}x} & \mathbf{0} \\ \frac{d}{dx} \mathbf{Q}(x) & \mathbf{M}e^{\mathbf{M}x} \end{bmatrix} \quad (\text{A.6})$$

from which we have

$$\frac{d}{dx} \mathbf{Q}(x) = \mathbf{T}^T \mathbf{T} e^{-\mathbf{M}x} + \mathbf{M} \mathbf{Q}(x) \text{ with } \mathbf{Q}(0) = \mathbf{0}$$

The solution of this differential equation at $x = 1$ is

$$\mathbf{Q}(1) = e^{\mathbf{M}} \int_0^1 e^{-\mathbf{M}x} \mathbf{T}^T \mathbf{T} e^{\mathbf{M}x} dx$$

Hence $\int_0^1 e^{-\mathbf{M}x} \mathbf{T}^T \mathbf{T} e^{\mathbf{M}x} dx = e^{-\mathbf{M}} \mathbf{Q}(1)$

Substitute $\mathbf{Q}(1)$ from the definition of $\mathbf{F}(x)$ to end the proof.

Appendix D: Numerical Formula for Computing LTE_n in (9)

From (9) and (10), we have

$$LTE_n = \left\| \mathbf{w}_n(\cdot) - \left(1 + \frac{h_n}{h_{n-1}} \right) \mathbf{w}_{n-1}(\cdot) + \frac{h_n}{h_{n-1}} \mathbf{w}_{n-2}(\cdot) \right\|$$

Using the definition in Appendix A, we can rewrite LTE_n as

$$LTE_n = \|\mathbf{L}\mathbf{y}(\cdot)\| = \|\mathbf{L} e^{\mathbf{L}x} \mathbf{y}(0)\|$$

where $\mathbf{L} = \begin{bmatrix} \mathbf{0} & \cdots & \mathbf{0} & (\frac{h_n}{h_{n-1}} \mathbf{I}) & (-\mathbf{I} - \frac{h_n}{h_{n-1}} \mathbf{I}) & \mathbf{I} \end{bmatrix}$

Applying the definition of the norm in (11), we obtain

$$LTE_n^2 = \mathbf{y}(0)^T \int_0^1 e^{2\mathbf{L}x} \mathbf{L}^T \mathbf{T}^T \mathbf{T} \mathbf{L} e^{2\mathbf{L}x} dx \mathbf{y}(0)$$

Apply the result of Lemma 1 and we have

$$LTE_n^2 = \mathbf{y}(0)^T \mathbf{Q} \mathbf{y}(0)$$

where $\mathbf{Q} = e^{-\mathbf{L}} \begin{bmatrix} \mathbf{0} & \mathbf{I} \end{bmatrix} e^{\begin{bmatrix} -\mathbf{L} & \mathbf{0} \\ \mathbf{L}^T \mathbf{T}^T \mathbf{T} \mathbf{L} & \mathbf{L} \end{bmatrix} x} \begin{bmatrix} \mathbf{I} \\ \mathbf{0} \end{bmatrix}$ and \mathbf{I} is an identity matrix with the same dimension as \mathbf{L} .

Appendix E: Numerical Formula for Computing ERR_i

Based on the definitions in Appendix A,

$$\text{let } \hat{\mathbf{y}}_n(x) = \begin{bmatrix} \hat{y}_n(x) \\ \hat{\mathbf{w}}_n(x) \end{bmatrix}, \hat{\mathbf{L}} = \begin{bmatrix} \mathbf{L} & \mathbf{0} \\ \mathbf{0} & \hat{\mathbf{M}}_i \end{bmatrix}$$

$$\text{and } \mathbf{L} = \begin{bmatrix} \mathbf{E}_n & -\mathbf{I} \end{bmatrix}$$

Then (A.1) and (13) can be combined to give

$$\hat{\mathbf{y}}_n(x) = e^{\hat{\mathbf{L}}(x-x_{i-1})} \hat{\mathbf{y}}_n(x_{i-1}) \text{ for } x_{i-1} \leq x \leq x_i$$

Also (20) can be formulated as

$$ERR_i^2 = \int_{x_{i-1}}^{x_i} [\mathbf{L} \hat{\mathbf{y}}_n(x)]^T \mathbf{T}^T \mathbf{T} [\mathbf{L} \hat{\mathbf{y}}_n(x)] dx$$

$$= \hat{\mathbf{y}}_n(x_{i-1})^T \int_{x_{i-1}}^{x_i} e^{\hat{\mathbf{L}}(x-x_{i-1})} \mathbf{L}^T \mathbf{T}^T \mathbf{T} \mathbf{L} e^{\hat{\mathbf{L}}(x-x_{i-1})} dx$$

$$\hat{\mathbf{y}}_n(x_{i-1})$$

$$= (x_i - x_{i-1}) \hat{\mathbf{y}}_n(x_{i-1})^T$$

$$\int_0^1 e^{\hat{\mathbf{L}}(x-x_{i-1})} \mathbf{L}^T \mathbf{T}^T \mathbf{T} \mathbf{L} e^{\hat{\mathbf{L}}(x-x_{i-1})} dx \hat{\mathbf{y}}_n(x_{i-1})$$

$$= (x_i - x_{i-1}) \hat{\mathbf{y}}_n(x_{i-1})^T \hat{\mathbf{Q}} \hat{\mathbf{y}}_n(x_{i-1}) \quad (\text{A.7})$$

$$\text{where } \hat{\mathbf{Q}} = e^{-\hat{\mathbf{L}}} \begin{bmatrix} \mathbf{0} & \mathbf{I} \end{bmatrix} e^{\begin{bmatrix} -\hat{\mathbf{L}} & \mathbf{0} \\ \mathbf{L}^T \mathbf{T}^T \mathbf{T} \mathbf{L} & \hat{\mathbf{L}} \end{bmatrix} x} \begin{bmatrix} \mathbf{I} \\ \mathbf{0} \end{bmatrix}$$

and \mathbf{I} is an identity matrix with the same dimension as $\hat{\mathbf{L}}$.



Panuwat Dan-klang received B.Eng. from Prince of Songkla University, Thailand in 1998 and M.Eng from Kasetsart University in 2005. Currently, he is Ph.D. student at Chulalongkorn University. His research interests include circuit simulation, digital IC design and wireless sensor network.



Ekachai Leelarasmee received his B.Eng. in EE from Chulalongkorn University, Thailand in 1974 and Ph.D. in EE from University of California, Berkeley, USA in 1982 under the sponsorship from The Anandamahidol Foundation. His Ph.D. dissertation, in which the Waveform Relaxation was first proposed and applied for time domain analysis of large scale MOS integrated circuits, had given him three prestigious recognitions: the 1983 IEEE Guillemin-Cauer Award, the 1982 IEEE/ACM Design Automation Conference Best Paper Award and the 1981 U.C. Berkeley D.J. Sakrison Memorial Prize. He is now an associate professor in the electrical engineering department of Chulalongkorn University and was the pioneering developer of Thailand's first circuit simulation program LEK that won two invention awards from National Research Council of Thailand in 1985 and 1988. His current research works are in circuit simulation program, Closed Caption TV system and VLSI designs.

Transient Simulation of Coupled Transmission Lines based on Piecewise Exponential Approximation of Voltage and Current Distributions

Panuwat Dan-klang, Ekachai Leelarasmee
 Chulalongkorn University, EE department
 Pathumwan, Bangkok 10330, Thailand
 email panuwat@digital.ee.eng.chula.ac.th
 Chulalongkorn University, EE department
 Pathumwan, Bangkok 10330, Thailand
 email ekachai.l@chula.ac.th

Abstract— An approach for the transient simulation of coupled transmission lines is described. By treating the line voltage/current distributions as state variables, the Telegrapher equation is transformed into an ordinary differential equation. This allows the use of Backward Differentiation Formulae to discretize the time derivatives, yielding a time domain companion model of the transmission line together with the formulae for calculating its local truncation error. As the distributions get more complicated with time, a novel technique to approximate these spatial voltage/current distributions in the form of multi-dimensional piecewise exponential function is thus proposed. This technique enables the line to be dynamically bisected until the approximation error is a small percentage of the computed local truncation error. Hence, this approach complies with the accuracy control of a standard circuit simulator.

Keywords: exponential approximation; piecewise interpolation; distribution state variable; transmission line

I. INTRODUCTION

The transmission line is an essential component in high speed circuits. A designer must be able to predict the its effects, i.e. reflection, dispersion, and crosstalk, on the circuit. Unfortunately, this is a difficult task because characteristics of a transmission line are defined by a set of partial differential equations involving both time and spatial derivatives. Over the past three decades, numerous methods have been proposed to determine these transient phenomena. They can be classified into four groups.

The first group of methods is based on replacing the transmission line with a cascade of lumped RLCG segments [1] [2]. This so-called segmentation method is popular because it uses basic components that can be readily implemented in a general circuit simulator. However, a large number of segments, e.g. 100, may be required to achieve high accuracy. This results in high computational complexity.

The second group of methods is based on model order reduction [3-5] in which a transmission line terminal

characteristics is modeled in the frequency domain by rational functions. Although being computationally efficient, the reduced order model is accurate only when the signal frequency falls within the intended range. The third group of methods is based on the convolution integral [6, 7]. This method suffers from poor computational complexity at long time intervals.

The last group of methods [8, 9], called the distribution state variable method, derives the time domain companion model of a transmission line in terms of its voltage /current distributions along the line at previous time point. It then approximates the distributions using piecewise linear functions in the spatial domain. However, it does not specify how to control the accuracy of approximation with respect to the local truncation error. Also, the piecewise linear function does not seem to fit well with the exponential behavior of the distribution.

In this work, a method that belongs to the distribution state variable approach is described. In comparison with previous methods, our method uses piecewise exponential functions to approximate the voltage/current distributions. It has a potential to achieve high accuracy using only a small number of pieces. Moreover, we have tied this approximation process with the local truncation error associated with the time domain companion model of the transmission line. Therefore, the companion model will be automatically adjusted to suit the user specified accuracy in a way that is similar to lumped capacitors and inductors.

The rest of the paper is organized as follows. Section 2 reformulates the transmission line equations in the form of a state equation involving the voltage/current distributions as the state variables. Section 3 describes the technique to approximate these distributions at a given time point with piecewise exponential functions in which a bisection scheme is used. Then two numerical examples are presented in Section 4 to illustrate the effectiveness of this new approach.

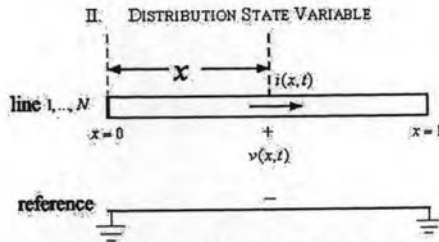


Figure 1. An N+1 coupled transmission line with unit length

Consider a set of N+1 coupled transmission lines with unit length as shown in Fig. 1. Let one line be treated as reference and the other N lines be characterized by the following Telegrapher Equation

$$\frac{\partial}{\partial x} \mathbf{w}(x,t) = -\mathbf{A} \frac{\partial}{\partial t} \mathbf{w}(x,t) - \mathbf{B} \mathbf{w}(x,t) \quad (1)$$

$$\mathbf{w}^T(x) = [\mathbf{v}(x,t)^T \quad \mathbf{i}(x,t)^T] : x \in [0,1]$$

$$\mathbf{A} = \begin{bmatrix} 0 & \mathbf{L} \\ \mathbf{C} & 0 \end{bmatrix}; \quad \mathbf{B} = \begin{bmatrix} 0 & \mathbf{R} \\ \mathbf{G} & 0 \end{bmatrix}$$

where $\mathbf{v}(x,t)$ and $\mathbf{i}(x,t)$ are vectors of N line voltages and N line currents, RLGC are N×N matrices associated with the per unit line characteristics. We now reformulate (1) as an ordinary differential equation in terms of a distributed state variable $\mathbf{w}(\bullet,t)$, i.e.

$$\frac{d}{dt} \mathbf{w}(\bullet,t) = \mathbf{F}(\mathbf{w}(\bullet,t))$$

where $\mathbf{F} \triangleq -\mathbf{A}^{-1}(\mathbf{B} + \mathbf{I} \frac{\partial}{\partial x})$. Applying the Backward Euler (BE) differentiation formula with timestep $h_n = t_n - t_{n-1}$ to approximate the time derivative at time t_n and letting $\mathbf{w}_n(\bullet) = \mathbf{w}(\bullet, t_n)$, we obtain

$$\frac{1}{h_n} [\mathbf{w}_n(\bullet) - \mathbf{w}_{n-1}(\bullet)] = \mathbf{F}(\mathbf{w}_n(\bullet)) \quad (2)$$

The local truncation error (LTE) incurred by the BE formula is

$$LTE_n = \|\mathbf{w}_n(\bullet) - \mathbf{w}(\bullet, t_n)\| = O(h_n^2) \quad (3)$$

where $\|\cdot\|$ is a norm defined as

$$\|\mathbf{w}(\bullet)\|^2 = \int_0^1 \mathbf{w}(x)^T \mathbf{Q}^T \mathbf{Q} \mathbf{w}(x) dx \quad (4)$$

with \mathbf{Q} being a non-singular matrix. The solution of (2) can be shown to be equivalent to solving

$$\frac{d}{dx} \mathbf{w}_n(x) = \mathbf{M}_n \mathbf{w}_n(x) + \mathbf{D}_n \mathbf{w}_{n-1}(x) \quad (5)$$

$$\text{where } \mathbf{M}_n = -\left(\frac{\mathbf{A}}{h_n} + \mathbf{B}\right); \quad \mathbf{D}_n = \frac{\mathbf{A}_n}{h_n}$$

The solution of (5) is given by

$$\mathbf{w}_n(x) = e^{\mathbf{M}_n x} \mathbf{w}_n(0) + \mathbf{J}_n(x) \quad (6)$$

where $\mathbf{J}_n(x) = \int_0^x e^{\mathbf{M}_n(x-\tau)} \mathbf{D}_n \mathbf{w}_{n-1}(\tau) d\tau$ is a constant

quantity at a time t_n . Let $x = 1$ and we obtain the relationship between the end point voltages and currents as

$$\mathbf{w}_n(1) = e^{\mathbf{M}_n} \mathbf{w}_n(0) + \mathbf{J}_n(1)$$

This relation describes the time domain companion model of the transmission line with respect to its terminals.

III. PIECEWISE EXPONENTIAL APPROXIMATION

Due to recursive relation in (2), $\mathbf{w}_n(x)$ will depend on $\mathbf{w}_i(x)$ for all $i=0, \dots, n-1$. This will progressively increase the complexity of computing $\mathbf{J}_n(1)$. To simplify this computation, we approximate $\mathbf{w}_n(x)$ with an exponential function, i.e.

$$\mathbf{w}_n(x) \approx \bar{\mathbf{w}}_n(x) = e^{\bar{\mathbf{M}}_n x} \bar{\mathbf{w}}_n(0) \quad (7)$$

where $\bar{\mathbf{M}}_n$ is chosen such that $\bar{\mathbf{w}}_n(x)$ interpolates $\mathbf{w}_n(x)$ at $2N+1$ points evenly distributed along the line, i.e.

$$\bar{\mathbf{w}}_n\left(\frac{k}{2N}\right) = \mathbf{w}_n\left(\frac{k}{2N}\right); \quad k = 0, 1, \dots, 2N \quad (8)$$

From (7) and (8), it can be deduced that

$$\bar{\mathbf{M}}_n = 2N \bullet \ln [\mathbf{W}_n \mathbf{W}_n^{-1}] \quad (9)$$

where $W_e = \left[w_n(\frac{i}{2N}); i=1, \dots, 2N \right]$

and $W_s = \left[w_n(\frac{i}{2N}); i=0, \dots, 2N-1 \right]$

For a simple case of two transmission lines ($N=1$), the exponential approximation reduces to

$$\tilde{M}_n = 2 \ln \left(\begin{bmatrix} v_n(\frac{1}{2}) & v_n(1) \\ i_n(\frac{1}{2}) & i_n(1) \end{bmatrix} \begin{bmatrix} v_n(0) & v_n(\frac{1}{2}) \\ i_n(0) & i_n(\frac{1}{2}) \end{bmatrix}^{-1} \right)$$

In order to accept $\tilde{W}_n(\cdot)$ as a good approximation of $W_n(\cdot)$, we must ensure that

$$Error_n = \|W_n(\cdot) - \tilde{W}_n(\cdot)\| \leq \alpha \cdot LTE_n$$

where α is a small number, e.g. $\alpha = 0.01$. If this condition is not satisfied, the line will be divided into two segments of equal length. Each separated segment is then exponentially approximated with its error calculated. The total approximation error is now the sum of these two errors. If the total error is still too large, the segment that has the largest error will be divided into two halves and the exponential approximation process is carried out with them. As a result, a bisection scheme is implemented and we obtain a piecewise exponential approximation of $W_n(x)$. Since the end points of each segment are points of interpolation, the approximated distribution is always continuous.

IV. NUMERICAL EXAMPLES

The circuit in the first example is shown in Fig. 2. The parameters of the transmission line are $L=1\text{mH/m}$, $C=10\mu\text{F/m}$, $G=0.2\text{ S/m}$ and $R=1\ \Omega/\text{m}$. The line is 1 meter long and starts with zero voltage/current distributions. Simulation is carried out using a fixed time step, i.e. $h_t = 1 \times 10^{-5}\text{ sec}$, and $\alpha = 1e-6$. The voltage waveform at the load-end ($x=1$) is shown in fig. 3. This waveform is indistinguishable from the case when $\alpha=0$, i.e. no piecewise exponential approximation is performed. Fig. 4 shows the number of exponential pieces required to approximate the distributions at various time points. We can see that the method automatically and dynamically divides the line into 11 segments while the unit step input wave travels in the line and gradually reduces the number of segments to 1 or 2 after the wave has reached the load. In comparison with the ideal case when there is no exponential approximation, the ideal distributions would consist of $(7 \times 10^{-4} / 10^{-5}) \times 2 = 140$ exponential terms at time $t = 7 \times 10^{-4}$. Therefore, a high

computational efficiency of this exponential approximation can be expected.

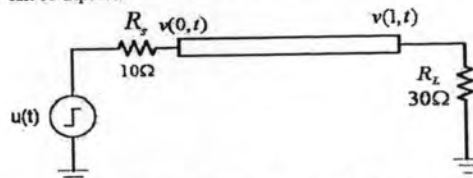


Figure 2. A single transmission line circuit with unit step input.

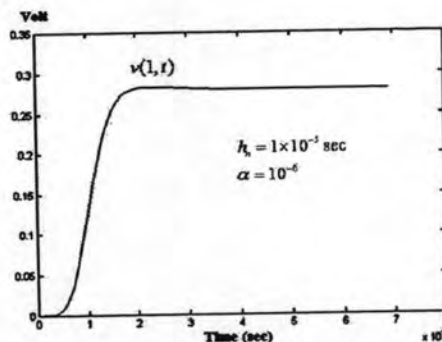


Figure 3. The voltage waveform at the load-end of the circuit in Fig. 2.

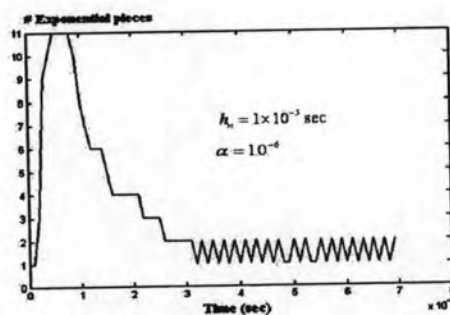


Figure 4. Variation of #exponential segments with time

The circuit in the second example, shown in Fig. 5, consists of three coupled transmission lines ($N=2$). The lines are 1 meter long with the following parameters

$$R = \text{diag}(10, 10) \Omega / \text{m} \quad G = \text{diag}(1, 1) \text{mS} / \text{m}$$

$$L = \begin{bmatrix} 100 & 25 \\ 25 & 100 \end{bmatrix} \text{nH} / \text{m} \quad C = \begin{bmatrix} 50 & -10 \\ -10 & 60 \end{bmatrix} \text{pF} / \text{m}$$

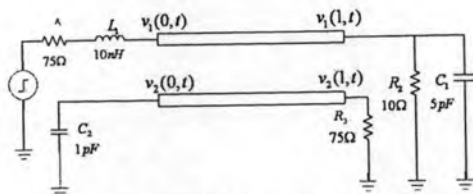


Figure 5. A circuit to demonstrate the coupling effect of transmission lines.

It is simulated using a fixed $0.2 nSec$ timestep and the approximation scale factor is $\alpha = 10^{-2}$. The simulated waveform coupled from line#1 to line#2 at the load-end is shown in Fig. 6 which is almost indistinguishable from the ideal situation. Fig. 7 shows the number of exponential segments used by the proposed approximation. It clearly illustrates the efficiency of the method since the maximum number of segments is only 5 which occurs only a few times while 2 or 1 segments are used most of the time.

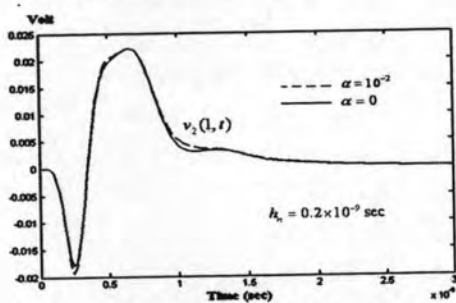


Figure 6. The coupled waveform at the load-end of line#2.

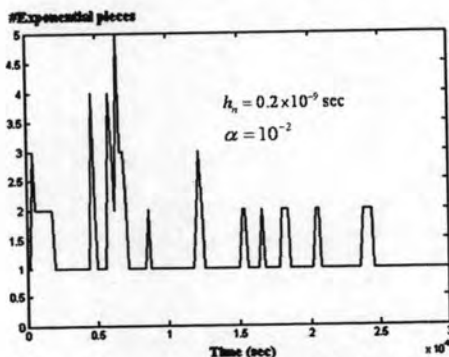


Figure 7. Variation of #exponential segment with time for the circuit in Fig. 5

V. CONCLUSION

The use of voltage/current distributions at previous time point for determining the time domain companion model of coupled transmission lines is described. These distributions can be approximated by piecewise exponential functions to simplify the computational complexity. The advantage of this approach is that accuracy can be controlled using the local truncation error that is typical in a standard circuit simulator.

VI. REFERENCES

- [1] H. W. Dommel, "Digital Computer Solution of Electromagnetic Transients in Single- and Multiphase Networks," *IEEE Transactions on Power Apparatus and Systems*, vol. PAS-88, pp. 388-399, 1969.
- [2] T. Dhaene and D. de Zutter, "Selection of lumped element models for coupled lossy transmission lines," *Computer-Aided Design of Integrated Circuits and Systems, IEEE Transactions on*, vol. 11, pp. 805-815, 1992.
- [3] S. K. Das and W. T. Smith, "Application of asymptotic waveform evaluation for analysis of skin effect in lossy interconnects," *Electromagnetic Compatibility, IEEE Transactions on*, vol. 39, pp. 138-146, 1997.
- [4] A. Odabasioglu, M. Celik, and L. T. Pileggi, "PRIMA: passive reduced-order interconnect macromodeling algorithm," *Computer-Aided Design of Integrated Circuits and Systems, IEEE Transactions on*, vol. 17, pp. 645-654, 1998.
- [5] D. Saraswat, R. Achar, and M. S. Nakhla, "Passive reduction algorithm for RLC interconnect circuits with embedded state-space systems (PRESS)," *Microwave Theory and Techniques, IEEE Transactions on*, vol. 52, pp. 2215-2226, 2004.
- [6] S. Lin and E. S. Kuh, "Transient simulation of lossy interconnects based on the recursive convolution formulation," *Circuits and Systems I: Fundamental Theory and Applications, IEEE Transactions on [see also Circuits and Systems I: Regular Papers, IEEE Transactions on]*, vol. 39, pp. 879-892, 1992.
- [7] Z. Tingdong, S. L. Dvorak, and J. L. Prince, "Lossy transmission line simulation based on closed-form triangle impulse responses," *Computer-Aided Design of Integrated Circuits and Systems, IEEE Transactions on*, vol. 22, pp. 748-755, 2003.
- [8] G. Yu-Shun, "Transient simulation of high-speed interconnects based on the semidiscretization of Telegrapher's equations," *Computer-Aided Design of Integrated Circuits and Systems, IEEE Transactions on*, vol. 21, pp. 799-809, 2002.
- [9] E. Leclaramco and P. Naenna, "A distributed state variables approach to the transmission lines transient simulation," 2004, pp. 73-76 vol.1

ประวัติผู้เขียนวิทยานิพนธ์

นายภาณุวัฒน์ ด้านกลาง เกิดวันที่ ๖ เมษายน พ.ศ. ๒๕๑๙ ที่จังหวัด กรุงเทพมหานคร สำเร็จการศึกษาปริญญาวิศวกรรมศาสตรบัณฑิต สาขาวิชาวิศวกรรมไฟฟ้า จาก คณะวิศวกรรมศาสตร์ มหาวิทยาลัยสงขลานครินทร์ ในปีการ ๒๕๔๑ และ ปริญญาวิศวกรรมศาสตรมหาบัณฑิต สาขาวิชาวิศวกรรมไฟฟ้า จากมหาวิทยาลัยเกษตรศาสตร์ ในปี ๒๕๔๗ และ สมัครเข้าศึกษาต่อในหลักสูตรวิศวกรรมศาสตรมหาบัณฑิต สาขาวิชาวิศวกรรมไฟฟ้า แขนง วิศวกรรมไฟฟ้าอิเล็กทรอนิกส์เชิงเลข ที่คณะวิศวกรรมศาสตร์ จุฬาลงกรณ์มหาวิทยาลัย ในปี การศึกษา ๒๕๔๘

หัวข้อวิทยานิพนธ์

การควบคุมความแม่นยำของการจำลองเชิงเวลาของวงจร
สายส่งโดยการประมาณค่าการกระจายแรงดันและกระแส
ในสายด้วยฟังก์ชันเลขชี้กำลังแบบแบ่งทอน

โดย

นาย ภาณุวัฒน์ ด้านกลาง

สาขาวิชา

วิศวกรรมไฟฟ้า

อาจารย์ที่ปรึกษาวิทยานิพนธ์หลัก

รองศาสตราจารย์ ดร. เอกชัย ลีลารัมย์

คณะวิศวกรรมศาสตร์ จุฬาลงกรณ์มหาวิทยาลัย อนุมัติให้บัณฑิตวิทยานิพนธ์ฉบับนี้เป็นส่วน
หนึ่งของการศึกษาตามหลักสูตรปริญญาตรีบัณฑิต

..... คณบดีคณะวิศวกรรมศาสตร์
(รองศาสตราจารย์ ดร. บุญสม เลิศหิรัญวงศ์)

คณะกรรมการสอบวิทยานิพนธ์

.....ประธานกรรมการ
(รองศาสตราจารย์ ดร. มนตรี สวัสดิ์ศฤงฆาร)

..... อาจารย์ที่ปรึกษาวิทยานิพนธ์หลัก
(รองศาสตราจารย์ ดร. เอกชัย ลีลารัมย์)

..... กรรมการ
(ผู้ช่วยศาสตราจารย์ ดร. ทับทิม อ่างแก้ว)

..... กรรมการ
(อาจารย์ ดร. คมสัน เพ็ชรรักษ์)

..... กรรมการภายนอกมหาวิทยาลัย
(ดร. สุเทพ ฉิมคล้าย)